

MASTER'S THESIS ABSTRACT

THE RELATIONSHIP BETWEEN SEA SURFACE TEMPERATURE
AND MAXIMUM INTENSITY OF TROPICAL CYCLONES
IN THE EASTERN NORTH PACIFIC OCEAN

by

Luke David Whitney, Captain, USAF

* * * * *

THE OHIO STATE UNIVERSITY

1995

Pages: 86 Degree Awarded: M.S.

Title		J
Author		
Subject		
Availability		
By		
Distribution		
Availability Codes		
Dist	Avail and/or Special	
A-1		

An empirical relationship between climatological sea surface temperature (SST) and maximum intensity of Eastern North Pacific tropical cyclones is developed from a 31-year sample (1963-1993). This relationship is compared with the relationship for Atlantic tropical cyclones developed in a similar study by DeMaria and Kaplan and with the theoretical results of Emanuel. Overall, Eastern North Pacific storms do not come as close to their maximum potential intensity (MPI) as do Atlantic storms. At the time of their maximum intensity, only 11% of Eastern North Pacific storms reach 80% or more of their MPI compared with 19% in the Atlantic. Poleward recurvature of Atlantic storms over cooler waters appears to be a major factor in the difference between the two empirical relationships. Storms that mature west of 110°W tend to reach a considerably higher fraction of their MPI than storms that reach their maximum intensity east of 110°W. Assuming the tropopause temperature is a function of SST, the theoretical results are in general agreement with the observations over SSTs of 24 to 28°C. During El Nino years, Eastern North Pacific storms reach their maturity at positions farther south and farther west than in non-El Nino years. Storms also tend to obtain a higher portion of their MPI and reach higher maximum intensities when the QBO is in its westerly phase.

MASTER'S THESIS ABSTRACT

THE OHIO STATE UNIVERSITY
GRADUATE SCHOOL

NAME: Whitney, Luke, David

QUARTER/YEAR: Spring/1995

DEPARTMENT: Atmospheric Science

DEGREE: M.S.

ADVISER'S NAME: Hobgood, Jay, S.

THESIS TITLE: The Relationship Between Sea Surface Temperature And Maximum
Intensity Of Tropical Cyclones In The Eastern North Pacific Ocean

An empirical relationship between climatological sea surface temperature (SST) and maximum intensity of Eastern North Pacific tropical cyclones is developed from a 31-year sample (1963-1993). This relationship is compared with the relationship for Atlantic tropical cyclones developed in a similar study by DeMaria and Kaplan and with the theoretical results of Emanuel. Overall, Eastern North Pacific storms do not come as close to their maximum potential intensity (MPI) as do Atlantic storms. At the time of their maximum intensity, only 11% of Eastern North Pacific storms reach 80% or more of their MPI compared with 19% in the Atlantic. Poleward recurvature of Atlantic storms over cooler waters appears to be a major factor in the difference between the two empirical relationships. Storms that mature west of 110°W tend to reach a considerably higher fraction of their MPI than storms that reach their maximum intensity east of 110°W. Assuming the tropopause temperature is a function of SST, the theoretical results are in general agreement with the observations over SSTs of 24 to 28°C. During El Nino years, Eastern North Pacific storms reach their maturity at positions farther south and farther west than in non-El Nino years. Storms also tend to obtain a higher portion of their MPI and reach higher maximum intensities when the QBO is in its westerly phase.

Jay S. Hobgood
Advisor

THE RELATIONSHIP BETWEEN SEA SURFACE TEMPERATURE
AND MAXIMUM INTENSITY OF TROPICAL CYCLONES
IN THE EASTERN NORTH PACIFIC OCEAN

A Thesis

Presented in Partial Fulfillment of the Requirements for
the Degree of Master of Science to the
Graduate School of The Ohio State University

by

Luke David Whitney, B.S.

* * * * *

The Ohio State University

1995

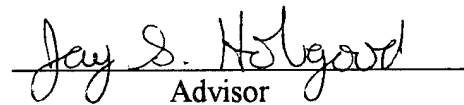
Master's Examination Committee:

Dr. Jay S. Hobgood

Dr. John N. Rayner

Dr. Jeffrey C. Rogers

Approved by


Advisor

Atmospheric Science Graduate Program

ACKNOWLEDGEMENTS

A great debt of gratitude is owed to my former commander, LtCol Richard W. Talyor, USAF, without whose help I would not have had the opportunity to attend Texas A&M University to pursue a BS in Meteorology and to write this note of appreciation as an attachment to my master's thesis--Thanks. Many thanks to my advisor, Dr. Jay Hobgood, for helping to secure a workable project and putting me in touch with the right people when it seemed like there was no beginning, for his constant enthusiasm for his chosen field of work, and for his many helpful comments to ensure this endeavor was a success. I would like to extend a sincere thank you to Dr. Mark DeMaria of the Hurricane Research Division in Miami, Florida who suggested the topic and supplied the necessary data for this research. The additional comments and suggestions provided by the other committee members, Dr. John Rayner and Dr. Jeff Rogers were also appreciated. Thanks also to Jeff Baars and Kevin Petty for taking time from their busy schedules to help with some computer graphics. I am indebted to the United States Air Force for taking a chance on my potential--may my service always be up to your standards. Finally, a special thank you to my wife Kim, and three children, Shelby, Trevor, and Travis, for enduring yet another step towards a brighter tomorrow.

VITA

January 19, 1958	Born - Sidney, New York
1979	U.S. Air Force Weather Specialist School
1979-1983	Weather Observer, McGuire Air Force Base, New Jersey and McClellan Air Force Base, California
1983	U.S. Air Force Weather Technician School
1984-1987	Weather Forecaster, USAF, Nevada
1989	B.S., Texas A&M University, College Station, Texas
1990-1993	Weather Forecaster and Command Weather Briefer for Headquarters, Air Combat Command, Langley Air Force Base, Virginia
1994-Present	Weather Officer, USAF, The Ohio State University, Columbus, Ohio

FIELDS OF STUDY

Major Field: Atmospheric Science

TABLE OF CONTENTS

ACKNOWLEDGEMENTS	ii
VITA	iii
TABLE OF CONTENTS	iv
LIST OF TABLES	vi
LIST OF FIGURES	viii
CHAPTER	PAGE
I. INTRODUCTION	1
II. LITERATURE REVIEW	3
III. DATA AND METHODOLOGY	16
3.1 Eastern North Pacific Best Track Data	16
3.2 Climatological SST Data	19
3.3 Elimination of Land Cases	20
3.4 Other Adjustments to the Data Base	21
3.5 Climatological SST Versus Tropical Cyclone Intensity	22
3.5.1 Intensity Curves	25
3.5.2 Development of the Empirical Maximum Intensity Function	28
3.6 Comparison of Empirical Results With Theory	29
3.7 Relative Intensity	32
3.8 Required Cooling	35
IV. ANALYSIS / RESULTS	37
4.1 Stratifying SST Data	37
4.2 Intensity Curves	40
4.3 Empirical Maximum Potential Intensity Function	42

4.3.1 Empirical Results Versus Theory	46
4.4 The Relative Intensity of Eastern North Pacific Tropical Cyclones	49
4.4.1 Distribution of Relative Intensity by Latitude and and Longitude	53
4.4.2 Stratification of Relative Intensity by Month	55
4.4.3 Stratification of Relative Intensity by Year	57
4.5 Relationship of El Niño and the QBO to Eastern North Pacific Tropical Cyclones	60
4.6 Required Cooling	63
V. SUMMARY / CONCLUSIONS	66
APPENDICES	
A. Maps of Montly Climatological SST for the Eastern North Pacific	71
B. Tables of SST Group Properties Stratified by Latitude and Longitude	80
LIST OF REFERENCES	83

LIST OF TABLES

TABLE	PAGE
1. SST group properties	24
2. Intensity Percentiles	26
3. Eastern Pacific storms containing the maximum intensity data points	27
4. Dvorak empirical relationship between the current intensity number, the maximum wind speed (MWS), and the minimum sea-level pressure (MSLP) in tropical cyclone (Dvorak, 1984). Values with an * by them are not from the original Dvorak scheme. They are added here as described in the text and are used to help convert wind speeds predicted by the EPMPI equation to pressures	30
5. Properties of SST groups when midpoints are placed at half degrees	39
6. SST group properties with first 4 observations of each storm eliminated	41
7. Relationship between the EPMPI function and outflow temperature based on the theory of Emanuel (1988). Minimum sea-level pressures (MSLP) from Dvorak (1984) have been interpolated where necessary	47
8. Average relative intensity (R.I.) of Eastern Pacific tropical cyclones from 1963 to 1993 stratified by latitude and longitude	54
9. Average relative intensity of Eastern North Pacific tropical cyclones stratified by month for the 31-year sample (1963 to 1993)	56
10. Stratification of the Eastern North Pacific Sample by El Niño and the phase of the QBO. El Niño years are the same as those in DK1. QBO years are the same as in Shapiro (1989), updated through 1992 by DK1. Entries in the 5 right-hand columns are based on the values when each storm reached its maximum intensity	61
11. SST Group Properties for Eastern North Pacific tropical cyclones at positions $\geq 18^\circ\text{N}$	81

12. SST Group Properties for Eastern North Pacific tropical cyclones at positions south of 18°N	81
13. SST Group Properties for Eastern North Pacific tropical cyclones at positions $\geq 110^{\circ}\text{W}$	82
14. SST Group Properties for Eastern North Pacific tropical cyclones at postions east of 110°W	82

LIST OF FIGURES

FIGURE	PAGE
1. Vertical instability as determined by the difference between the temperature of the air lifted adiabatically from the sea surface to 300 mb and the average air temperature at 300 mb over the North Atlantic ocean in September (Palmén, 1948)	5
2. Same as figure 1 except for the month of February	5
3. Typical hurricane paths originating over regions where the SST is generally greather than 26°C during the warmest season (Palmén, 1948)	6
4. Miller's (1958) relationship between sea surface temperature and maximum potential intensity of tropical cyclones (from Elsberry <i>et al.</i> , 1987)	6
5. Change in central pressure versus sea surface temperature for Hurricane Esther (Perlroth, 1962)	8
6. Scatter diagram of maximum sustained wind speed (MSW) corrected for storm motion versus climatological SST for a 12-year sample of Atlantic tropical cyclones. The curve drawn against the data represents the SST capping function based on the 99th percentile. (Merrill, Fig. 3, 1987)	10
7. The maximum storm intensity and the 99th, 95th, 90th, and 50th intensity percentiles versus SST from DeMaria and Kaplan (1994a). Intensities have been corrected for storm translational speed. The period of record is 1962 to 1992	14
8. The observed maximum storm intensity for each 1°C SST group and the least-squares function fit for the 31-year Atlantic sample (DeMaria and Kaplan, 1994a)	14

9. Scatter diagram showing the intensity and SST of all 11,062 observations in the 31-year sample (1963-1993). Intensities are corrected for storm translational speed	23
10. Intensity curves for the Eastern North Pacific with land cases removed and intensities corrected for storm translational speed	26
11. Graphical representation of the minimum sustainable central pressure (mb) of tropical cyclones as a function of SST (T_s) and outflow temperature (T_o) assuming ambient surface relative humidity of 80%. (Emanuel, 1988)	31
12. Position of each of the 467 tropical cyclones in the 31-year sample at the time it reached its maximum intensity	34
13. Tracks of Eastern North Pacific tropical cyclones from 1980-1989. Cyclones originate east of the line in (a), between the lines in (b) and (c), and west of the line in (d). The symbol (X) marks the average initial location for each group. (Zehnder, 1993)	34
14. Fit of maximum intensity curve to actual data using SST groups in Table 1	38
15. Fit of maximum intensity curve to actual data using SST groups in Table 5	38
16. The EPMPI function and the maximum intensity data from each SST group	44
17. Comparison of best-fit lines with and without the 29°C SST group and the maximum intensity data	44
18. Comparison between the Eastern North Pacific MPI and Atlantic MPI functions	45
19. The required outflow temperature as a function of SST needed to make the theoretical maximum intensity equal to the empirical maximum potential intensity for Eastern North Pacific tropical cyclones	48
20. The number of Eastern North Pacific tropical cyclones per 5% interval of relative intensity	51
21. Same as figure 20 except for the Atlantic (from DK1)	51

22. Cumulative distribution of relative intensity (R.I.) for the Eastern North Pacific	53
23. Average relative intensities of Eastern North Pacific tropical cyclones for each year from 1963 to 1993	59
24. 5-Year running means of average relative intensity for the 31-year Eastern North Pacific sample (1963 to 1993)	59
25. Percentage of cases per 1°C increments of required cooling. Required cooling is the drop in SST needed to raise the average relative intensity to 100%	64
26. Climatological sea surface temperatures for the month of May	72
27. Climatological sea surface temperatures for the month of June	73
28. Climatological sea surface temperatures for the month of July	74
29. Climatological sea surface temperatures for the month of August	75
30. Climatological sea surface temperatures for the month of September	76
31. Climatological sea surface temperatures for the month of October	77
32. Climatological sea surface temperatures for the month of November	78
33. Climatological sea surface temperatures for the month of December	79

CHAPTER I

INTRODUCTION

In recent years, increasing emphasis has been placed on determining factors related to tropical cyclone intensity and intensity changes. Several studies have investigated the nature of the relationship between the sea surface temperature (SST) and maximum intensity of tropical cyclones. There exists both theoretical and empirical evidence that the SST provides an upper bound on the maximum intensity that a tropical cyclone can obtain. However, the majority of tropical cyclones never reach their theoretical or empirical upper limit in intensity. Past studies utilizing the idea of an upper limit on intensity have primarily applied it to tropical cyclones in the Atlantic and Western Pacific basins. DeMaria and Kaplan (1994a) developed an empirical relationship between climatological SST and the maximum intensity of tropical cyclones in the North Atlantic basin. This relationship was put to use in the recently developed Statistical Hurricane Intensity Prediction Scheme (SHIPS) model for the Atlantic basin (DeMaria and Kaplan, 1994b). This researcher has found no study that looked at how close the intensity of Eastern Pacific tropical cyclones have come to their theoretical or empirical upper bound. There is some speculation (DeMaria, personal communication, 1994) that Eastern Pacific tropical cyclones come much closer to their upper bound than storms in other basins.

The main purpose of this study is to investigate the relationship between SST and the maximum intensity of tropical cyclones in the Eastern North Pacific. The work of DeMaria and Kaplan (1994a) is closely paralleled. An empirical relationship between

climatological SST and maximum intensity is developed from a 31-year sample (1963-1993) of Eastern North Pacific tropical cyclones. The empirical results are compared with the theoretical results of Emanuel (1988) and with the empirical relationship between climatological SST and maximum intensity found for a 31-year sample of Atlantic tropical cyclones by DeMaria and Kaplan (1994a). The likelihood that a given storm will reach a set fraction of its maximum potential intensity is determined using the empirical relationship developed for the Eastern North Pacific. In addition, the tropical cyclones in the 31-year sample are examined at the time they reached their maximum observed intensity. The sensitivity of tropical cyclone intensification to SST is also looked at.

In this study, the words storm and tropical cyclone are used interchangeably and refer to tropical cyclones that have obtained at least tropical storm strength ($>17 \text{ m s}^{-1}$) or greater at sometime during their life cycle. Chapter 2 is a brief review of previous literature on the subject of the relationship between SST and tropical cyclone development and intensity. The tropical cyclone and climatological SST data, along with the overall methodology for this study, are discussed in chapter 3. Chapter 4 presents the analysis and results of this study. Concluding remarks are given in chapter 5. It is hoped that this study will have some application to the prediction of tropical cyclone intensity in the Eastern North Pacific and possibly elsewhere.

CHAPTER II

LITERATURE REVIEW

Over the past few decades, the primary emphasis in tropical cyclone forecasting has focused on improving track predictions. As progress in tropical cyclone track prediction has slowed, increasing attention has been paid to factors related to tropical cyclone intensity and to predicting intensity changes. The external environment appears to be a key ingredient in tropical cyclone intensification (Elsberry *et al.*, 1988). The strength of the vertical shear of the horizontal wind may indicate whether a tropical cyclone will intensify or weaken. Internal factors such as eye size (Holiday and Thompson, 1979) and concentric eyewall development (Willoughby *et al.*, 1982) are thought to be connected to intensity changes. Recent theoretical studies (Emanuel, 1988) and empirical research (DeMaria and Kaplan, 1994a) support the notion that sea surface temperature (SST) is linked to the maximum intensity obtainable in a tropical cyclone. It is hypothesized that the intensity of a tropical cyclone should increase with increasing SST. The following literature review focuses primarily on the relationship of SST to tropical cyclone intensity.

It has long been accepted that the primary energy source for tropical cyclone development and maintenance is the release of latent heat of condensation (Miller, 1958; Malkus and Riehl, 1960; Emanuel, 1986). It can also be said that the ocean is the primary source of energy (Merrill, 1988) since the ocean provides the necessary water vapor for condensation through evaporation from the sea surface. Emanuel (1986) stated that numerical simulations and observations of tropical cyclones indicate that evaporation from

the ocean surface is vital to the development of storms of reasonable intensity. Numerical simulation has shown that only a weak circulation results when evaporation from the ocean is neglected (Ooyama, 1969). As evaporation increases, the amount of available energy also increases and the potential for release of latent energy through condensation becomes greater. Factors that influence evaporation are the wind speed, degree of saturation of the air, air temperature above the water, and SST. All other factors being equal, the warmer the SST the higher the evaporation rate (Ahrens, 1991). This argument supports the hypothesis that tropical cyclone intensity should increase over warmer waters.

Palmén's (1948) study of the Atlantic found that vertical instability was a necessary condition for tropical hurricane formation. He computed vertical instabilities over the North Atlantic for the months of September (Fig. 1) and February (Fig. 2) assuming the atmosphere is barotropic at 300 mb and the surface air temperature is the same as the SST. Figures 1 and 2 clearly indicate that vertical instability is significantly greater in September when ocean waters are warmer. Palmén compared his vertical instability results with Atlantic SSTs and concluded that hurricanes form only in regions where the SST is greater than 26°C to 27°C . This conclusion is widely accepted and is supported by figure 3 which shows typical hurricane paths originating over ocean waters warmer than 26°C . Emanuel (1986) argued that the reason tropical cyclones did not form when SST was less than 26°C was due to the lack of vast deep conditional instability over parts of the ocean where SST was below this value. Palmén believed that vertical instability and warm SSTs were necessary but not sufficient conditions for hurricane formation.

Miller (1958) concluded that the minimum surface pressure of a hurricane is tied to the temperature of the sea surface over which it moves. By assuming hydrostatic equilibrium and using the equation of state, Miller found that the minimum possible surface pressure is a function of the SST, the surface air relative humidity, the dominant lapse rates in the

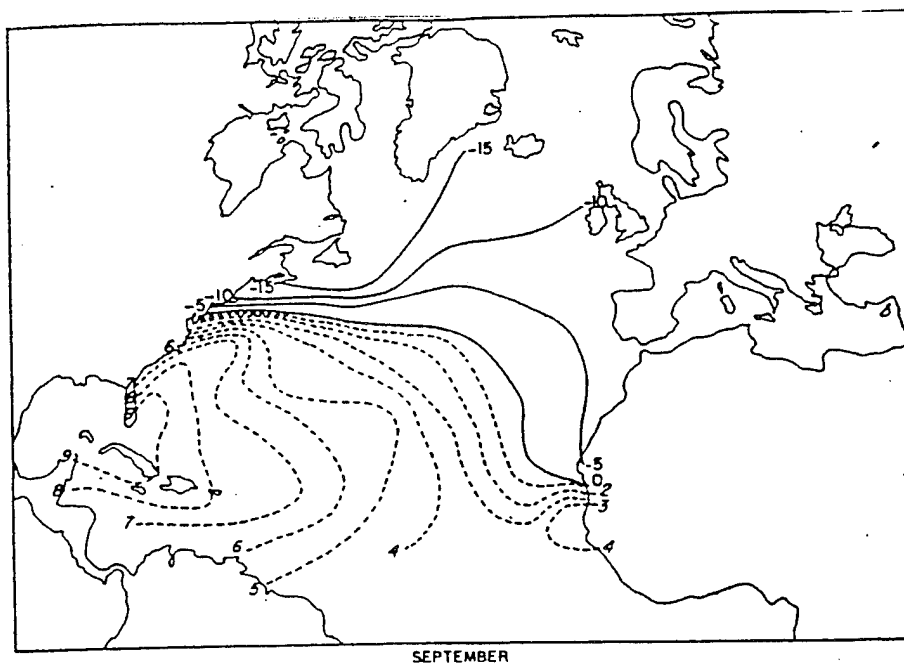


Fig. 1. Vertical instability as determined by the difference between the temperature of the air lifted adiabatically from the sea surface to 300 mb and the average air temperature at 300 mb over the North Atlantic ocean in September. (Palmén, 1948)

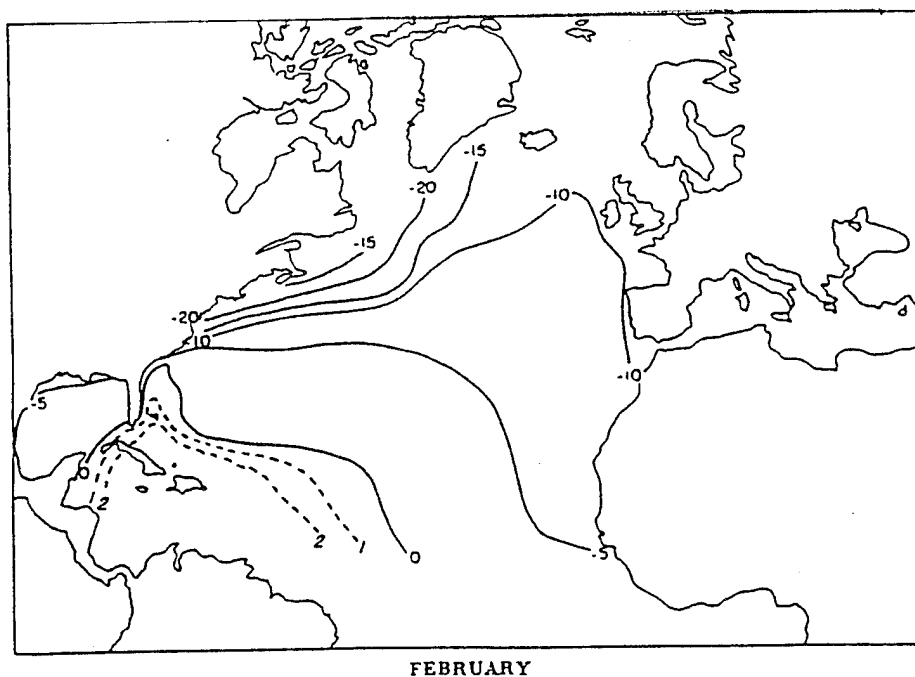


Fig. 2. Same as figure 1 except for the month of February.

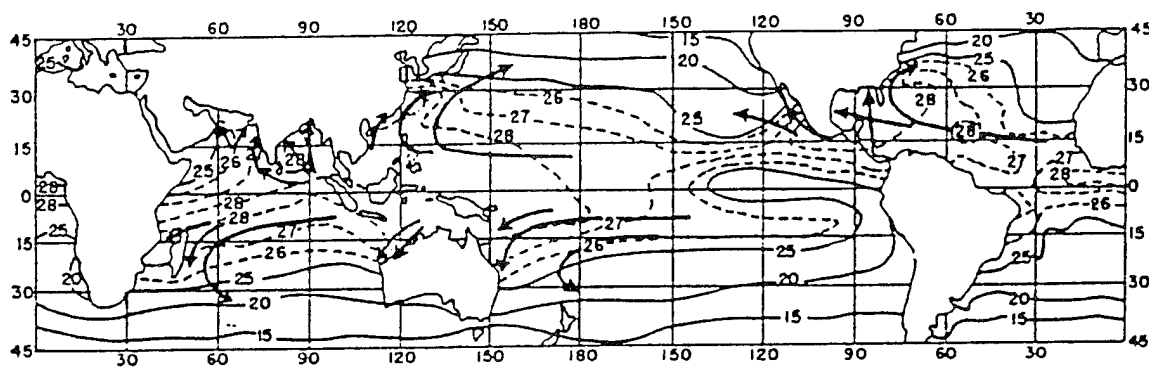


Fig. 3. Typical hurricane paths originating over regions where the SST is generally greater than 26°C during the warmest season. (Palmén, 1948)

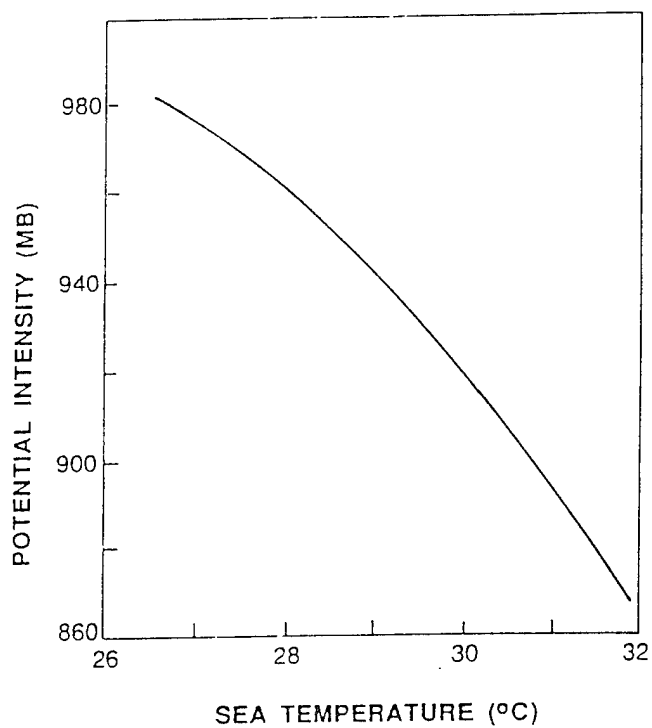


Fig. 4. Miller's (1958) relationship between sea surface temperature and maximum potential intensity of tropical cyclones. (from Elsberry *et al.*, 1987)

storm region, and the height and potential temperature at the top of the hurricane circulation (Miller, 1958). The temperature reached at the top of the tropical cyclone vortex is considered to be partially dependent upon the SST. Miller determined the minimum surface pressure could be obtained by lifting air moist adiabatically from the surface to near the tropopause and then subsiding it dry adiabatically back to the surface in the eye. Below 10 km, Miller accounted for sufficient mixing between the eye and the eyewall to preserve realistic humidities in the eye. Elsberry *et al.* (1987) points out that Miller calculated the maximum intensity possible in a tropical cyclone, for realistic SSTs, to be 860 mb; the most intense tropical cyclone on record is Typhoon Tip with a minimum pressure of 870 mb. The result of Miller's calculations of minimum pressures over a range of SSTs is shown in Fig. 4.

Miller understood that the results shown in Fig. 4 could only occur under ideal conditions and that very few storms actually reach their maximum potential intensity. Miller agreed with Palmén that warm SSTs are a necessary but not sufficient condition for intense tropical storm development. Miller suggested that tropical cyclone intensity is determined primarily by circulation features around the tropical cyclone and that the SST provides an upper limit on the intensity.

In a study of eleven Atlantic hurricanes, Fisher (1958) found considerable evidence that hurricanes develop over relatively warm ocean waters and are disposed to weaken as they move over colder water. A similar but more detailed study of hurricane Esther (1961) by Perlroth (1962) supported Fisher's findings. Using empirically constructed SST charts overlaid with the track of hurricane Esther, Perlroth noted that changes in the hurricane's intensity were apparently strongly related to the SST over which it moved. Figure 5 shows how hurricane Esther's central pressure varied with changing SST. Perlroth's analyses showed that Esther's central pressure fell when moving from colder to warmer water and rose when moving from warmer to colder water. Perlroth (1962) stressed that

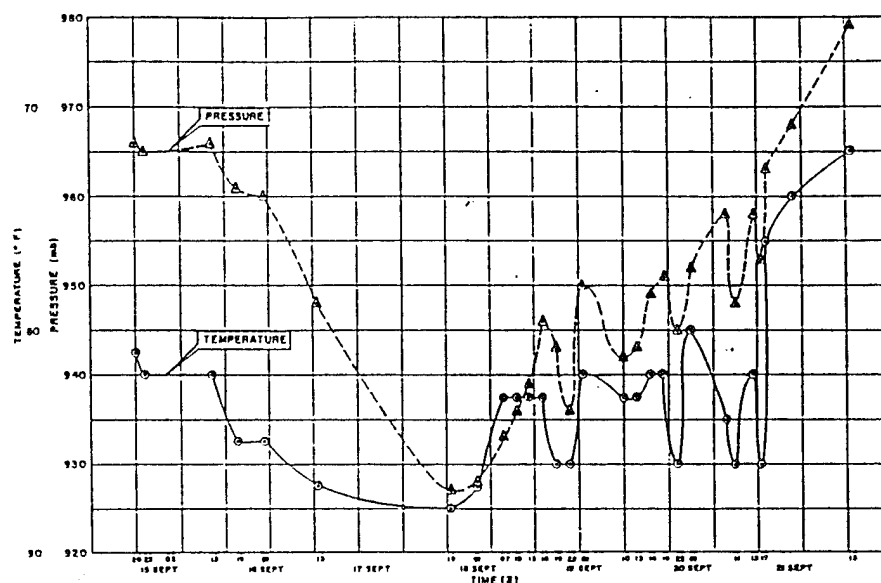


Fig. 5. Change in central pressure versus sea surface temperature for Hurricane Esther (Perlroth, 1962).

the apparent relationship between intensity and SST holds under the assumptions that the hurricane retains its tropical characteristics and does not interact with a front or extratropical trough.

Malkus and Riehl (1960) derived an expression relating decreases in the surface pressure to increases in the equivalent potential temperature. They determined that moist adiabatic ascent by convective activity to the top of the convective layer is not sufficient enough to reduce the surface pressure much below 1000 mb by the hydrostatic equation. Haurwitz (1935) found that surface pressures in hurricanes were close to being hydrostatic. Malkus and Riehl concluded that a local heat source was necessary in order for surface pressures to reach the low values typically found in hurricanes. Assuming a mean tropical atmosphere with an undisturbed top at 100 mb and moist adiabatic ascent,

Malkus and Riehl (1960) found that sea-level pressure (p_s) and equivalent potential temperature (θ_e) were linearly related by

$$-\delta p_s \text{ (mb)} = 2.5 \delta \theta_e \text{ (°K)} \quad (1)$$

Palmén and Newton (1969) claim that with typical saturation deficits at the surface, θ_e changes by approximately 4.4 °K for every 1°C change in surface temperature (T_s). Thus equation (1) was rewritten as

$$-\delta p_s \text{ (mb)} = 11 \delta T_s \text{ (°C)} \quad (2)$$

Equation (2) predicts an 11 mb decrease in pressure for every 1°C increase in SST.

Merrill (1987, 1988) compared climatological SST with tropical cyclone intensity, as measured by maximum sustained winds, for a sample of Atlantic hurricanes and found evidence of an empirical potential intensity relationship between the two factors. This relationship suggests that as SST increases the maximum potential intensity also increases. Figure 6 shows the scatter plot of maximum sustained wind, corrected for storm motion, versus SST from Merrill (1987). Merrill (1987) suggested that since a wide range of intensities are observed for a given SST, that the SST was better treated as a capping function on the tropical cyclone intensity rather than as a direct predictor. Merrill's studies support Miller's (1958) conclusion that SST may provide an upper bound on the maximum potential intensity of tropical cyclones. Merrill also agreed that environmental interactions were the main reason the majority of tropical cyclones failed to reach their maximum potential intensity.

Emanuel (1986) developed an expression for computing the minimum attainable central surface pressure in a tropical cyclone as a function of surface air temperature and outflow temperature. Emanuel found the minimum central surface pressure to be highly sensitive

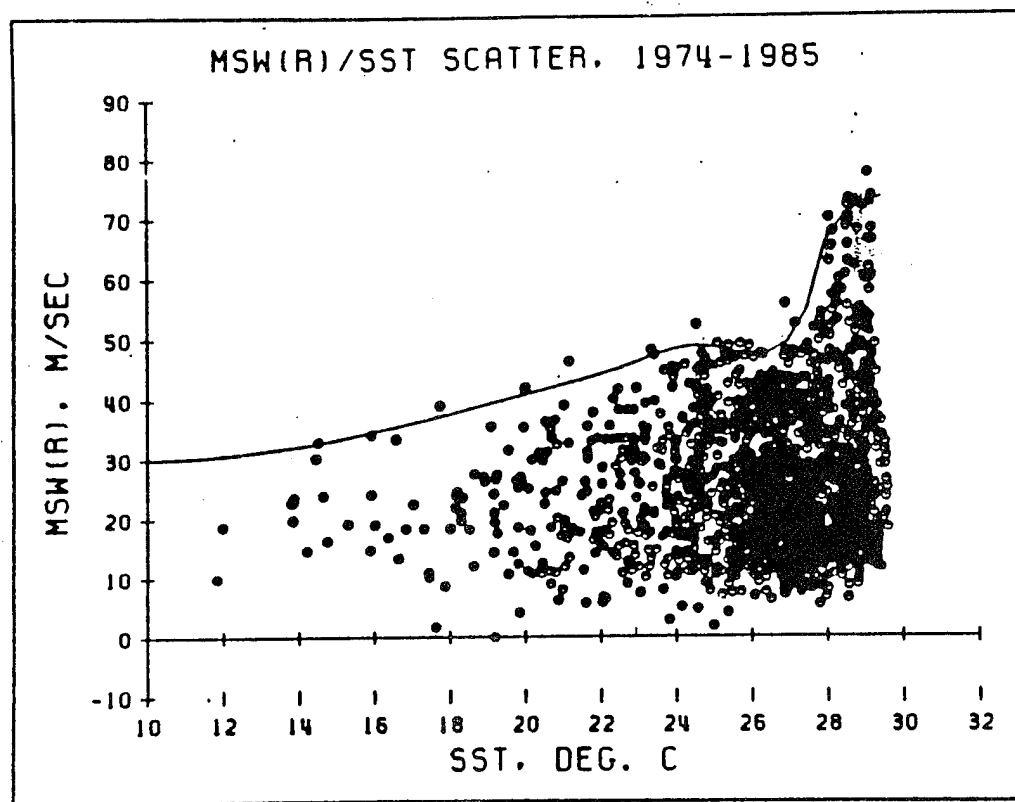


FIG. 6. Scatter diagram of maximum sustained wind speed (MSW) corrected for storm motion versus climatological SST for a 12-year sample of Atlantic tropical cyclones. The curve drawn against the data represents the SST capping function based on the 99th percentile. (Merrill, Fig. 3, 1987).

to surface air temperature and, to some degree, the outflow temperature. It is suggested that the surface air temperature over the ocean is typically within 1°C to 2°C below the SST (Riehl, 1954). The point here is that the surface air temperature over the ocean is generally very close to the SST. In some studies the SST is used in place of the surface air temperature (e.g., Palmén, 1948; Reid and Gage, 1981; Emanuel, 1986). Emanuel (1986) looked at the difference between the ambient 300 mb temperature and the temperature of a parcel lifted adiabatically from 1000 to 300 mb, plotted as a function of SST. Emanuel supported the earlier work of Palmén by concluding that deep conditional instability was necessary for tropical cyclone formation and that SSTs greater than 26°C to 27°C were required for this to occur.

Emanuel (1988) derived a theory relating maximum hurricane intensity to SST by representing the hurricane as a Carnot engine. This theory predicted an upper bound on the hurricane intensity based on SST, supporting earlier studies. A comparison of peak intensities of hurricanes predicted by the theory to those found in actual hurricanes under the same conditions indicated that most hurricanes do not reach their theoretical maximum intensity. It is suggested that only the most intense hurricanes come close to their theoretical upper limit (Emanuel, 1988). Emanuel did not take into account negative environmental influences, such as strong vertical wind shear or upwelling, which would hinder the hurricane from reaching its theoretical maximum intensity.

Upwelling in the wake of a tropical cyclone may significantly lower the SST (Leipper, 1967; Price, 1981). Leipper's (1967) observations of SST in the wake of hurricane Hilda, 1964, suggests that upwelling lowered the SST by as much as 6°C along the track of the storm. Other studies (e.g., Fedorov *et al.*, 1979; Pudov *et al.*, 1979; Wright, 1969; Jordan, 1964), in addition to Leipper's study, reveal a range of SST responses between -1 to -6°C due to upwelling (Price, 1981). Price (1981) compared the results of the above studies and found the decrease in SST due to upwelling appears to be enhanced for slower

moving storms ($\leq 4 \text{ m s}^{-1}$) and for storms of greater strength. Price suggested that a large decrease in SST could significantly reduce evaporation and consequently have an adverse effect on hurricane strength. Schade (1993) also found that SST feedback, due to upwelling in the wake of the storm, can have a negative impact on hurricane intensity, especially for slower moving storms. Using a coupled hurricane-ocean model, Schade (1993) determined that the SST feedback may explain a weakening in storm intensity of up to 44 mb. Schade concluded that SST was a major factor affecting a hurricane's intensity.

Evans (1993) tested the theory relating maximum hurricane intensity and SST using observational data for a 20-year period covering five ocean basins (North Atlantic, western North Pacific, South Pacific-Australian region, north Indian and southwest Indian oceans). The results from this study agreed with Merrill (1988) in concluding that SST alone is not a sufficient predictor of tropical cyclone intensity and that other factors must play a more dominant role in determining a storm's intensity. Inspection of Evans's (1993) scatter diagrams of maximum storm intensity versus SST indicate that the most intense storms generally occur over the warmer waters in the 28°C SST group or higher. However, Evans supported her claim that SST is not the limiting factor on tropical cyclone intensity by stating the fact that a wide range of intensities are observed for the 25°C and higher SST groups. Evans did acknowledge that SST may provide an upper limit to tropical cyclone intensity.

DeMaria and Kaplan (1994a) extended the work of Merrill (1987) by developing an empirical relationship between climatological SST and the maximum intensity of Atlantic tropical cyclones from a 31-year sample (1962-1992). Maximum wind speed was used as the measure of maximum observed intensity. Every 6-hour observation of intensity for each storm in the sample was assigned to one of 16 evenly spaced (1°C intervals) SST groups ranging from 14.5°C to 30.5°C . The storm translational speed was subtracted

from the intensity and the resulting maximum wind for each group was plotted against the midpoint of each SST group (15.0°C to 30.0°C). In addition the 99th, 95th, 90th, and 50th intensity percentiles were determined. Figure 7 shows the maximum and percentile intensity curves from DeMaria and Kaplan (1994a). A function was then fit to the maximum intensity found in each SST group (Fig. 8). The result was an exponential function of the form

$$V = A + B \exp[C(T - T_0)], \quad (3)$$

where V represents the maximum wind, or maximum potential intensity (MPI) in m s^{-1} , T is the SST ($^{\circ}\text{C}$), T_0 is a reference temperature (30.0°C), and A , B , and C are constants ($A = 28.2 \text{ m s}^{-1}$; $B = 55.8 \text{ m s}^{-1}$; $C = 0.1813 \text{ }^{\circ}\text{C}^{-1}$). The above empirical formula supports the results of Miller (1958) and Emanuel (1988) by predicting significant increases in MPI with increasing SST. Implicitly included in the empirical formula is a relationship between SST and outflow temperature (DeMaria and Kaplan, 1994a). Under the assumption that the tropopause temperature is a function of SST, the theoretical results of Emanuel (1988) were found to be in agreement with observations over a wide range of SSTs (DeMaria and Kaplan, 1994a).

By comparing specific relative intensities to the fraction of cases reaching those relative intensities, DeMaria and Kaplan (1994a) determined that for the sample with land cases removed, 58% of storms reached 50% of their MPI, while only 19% reached 80% of their MPI. Relative intensity is the observed maximum intensity divided by the MPI as computed from the empirical formula (3) above. The results of their study agree with those of previous studies in suggesting that the SST is not the limiting factor on tropical cyclone intensity. Vertical shear of the horizontal wind and negative ocean response to

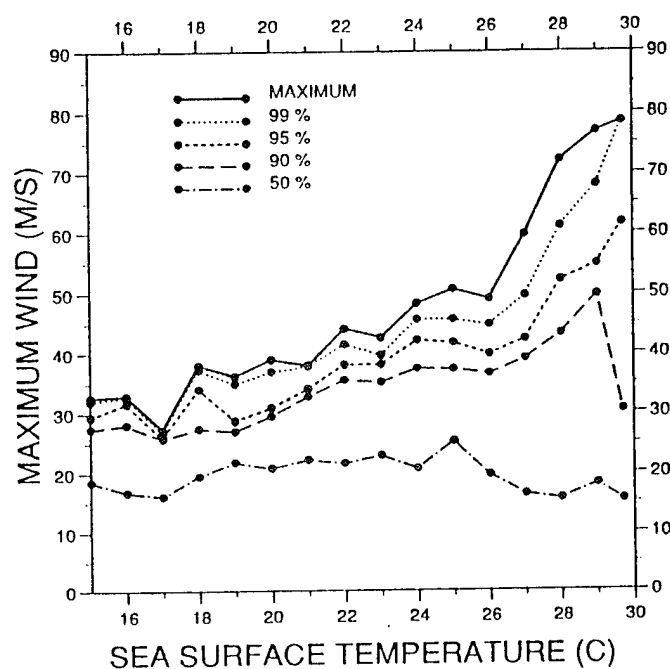


FIG. 7. The maximum storm intensity and the 99th, 95th, 90th, and 50th intensity percentiles versus SST from DeMaria and Kaplan (1994a). Intensities have been corrected for storm translational speed. The period of record is 1962-1992.

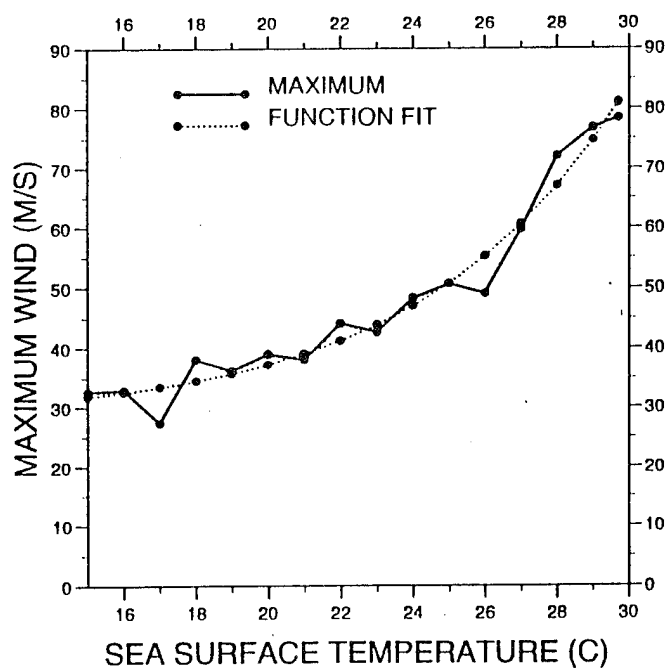


FIG. 8. The observed maximum storm intensity for each 1°C SST group and the least-squares function fit for the 31-year Atlantic sample (DeMaria and Kaplan, 1994a).

the tropical cyclone circulation were given as possible explanations of why some storms may not reach their MPI. This recent work by DeMaria and Kaplan supports the previous work of Merrill (1987, 1988) and others by indicating that the SST provides an upper limit on the maximum intensity of tropical cyclones.

DeMaria and Kaplan (1994b) put their empirical formula relating climatological SST to maximum intensity of hurricanes to work in the recently developed statistical hurricane intensity prediction scheme (SHIPS) model for the Atlantic basin. The MPI was used in calculating one of the seven synoptic predictors in the SHIPS model. They found the difference between the MPI and the current storm intensity, referred to as intensification potential (POT), is a better predictor of intensity change than the SST alone. POT is considered to be one of the three most important predictors used in the model. The SHIPS model has shown skill in the prediction of tropical cyclone intensity change and appears to be an improvement over the current statistical hurricane intensity forecast (SHIFOR) used by the National Hurricane Center (NHC).

The above studies all agree that the sea surface temperature may provide an upper limit on the maximum potential intensity obtainable in a tropical cyclone. There is argument over just how large a role SST plays in determining the actual maximum intensity a tropical cyclone reaches. Certainly, other factors interacting with the tropical cyclone will influence its intensity (Miller, 1958; Merrill, 1988; Evans, 1993; DeMaria and Kaplan, 1994a). It is possible that the relationship between SST and tropical cyclone intensity varies between ocean basins.

CHAPTER III

DATA AND METHODOLOGY

The methodology for this study was fairly straight forward and closely parallels the recent work of DeMaria and Kaplan (1994a) (from this point on referred to as DK1) which resulted in an empirical relationship (eq. 3) between climatological SST and maximum potential intensity for Atlantic tropical cyclones. DeMaria and Kaplan's MPI equation was later used in the development of the SHIPS model which is used to predict intensity changes in Atlantic tropical cyclones. The purpose of this study was to formulate an empirical relationship between climatological SST and maximum potential intensity for Eastern North Pacific tropical cyclones and to compare this relationship with that found in the Atlantic (DK1) and with the theoretical findings of Emanuel (1988). The author hopes that the empirical relationship determined for Eastern North Pacific tropical cyclones will be useful in developing a statistical hurricane intensity prediction scheme for the Eastern North Pacific basin in the near future.

3.1 Eastern North Pacific Best Track Data

The data used for this study was obtained from the Hurricane Research Division in Miami, Florida and consists of the Eastern North Pacific best track data file and a file of monthly climatological SSTs for the Eastern Pacific basin. The Eastern North Pacific best track file contains records of the positions and intensities of all Eastern North Pacific

tropical cyclones dating from 1949 to the present. Positions and intensities are recorded at 6-hour intervals. The reliability of intensity estimates prior to 1963 is somewhat in doubt since satellite data was not yet available. Because of this, the period from 1963 to 1993 was decided upon for this study. This 31-year period coincides well with the 1962-1992 period used for the Atlantic study by DK1.

In order to focus this study only on the Eastern North Pacific, all storms and observations in the best track file west of 140°W longitude were eliminated. The 140°W longitude line was chosen since it marks the border of the National Hurricane Center's area of responsibility in the Eastern North Pacific. Gray (1968) found that tropical cyclones in the Eastern North Pacific over a 20-year period were initially detected well east of 140°W. The same study also showed that over a 17 year period, all Eastern North Pacific tropical storms that acquired hurricane intensity did so at positions east of 140°W. Gray's findings appear to hold for this study since only 1,796 of the original 13,068 observations in the Eastern Pacific best track file from 1963 to 1993 were located west of 140°W. Three Central North Pacific storms (Ema-1982, Lala-1984, Iniki-1992) were eliminated since they did not maintain or acquire tropical storm strength while east of 140°W. In addition, storm record number 302 (Unnamed-1975) was also deleted because only one observation in the storm's history was reported east of 140°W.

Several other adjustments to the best track file were also made. For example, the very last observation in the records of tropical storm Marty (1991) and Ignacio (1991) were deleted since no maximum wind speed was reported. Hurricane Dolores (1985) had an incorrectly entered longitude on 07/01/1800Z (no decimal place was entered). A new longitude was obtained for this record by interpolating between the 07/01/1200Z and 08/01/0000Z observations. Other changes made to the Eastern North Pacific best track file are discussed where appropriate.

The maximum 1-minute sustained surface wind is used as the measure of intensity. Surface sea-level pressures were not used to represent intensity in this study since they were not routinely reported in the data base until 1988. In keeping with the DK1 study, the translational speed of each storm at each 6-hour position was calculated and then subtracted from the maximum wind estimate to obtain the storm relative wind speed. This was done to eliminate the possibility of having abnormally high maximum wind speeds caused by a few very fast moving storms. The translational speed for the first (last) observation of each storm was determined by calculating the distance between the first and second (last and next to last) position reports in the storm's record. The distance was then divided by the time interval between observations (6 hours) to obtain the storm's translational speed. For the observations between the first and last, the distance between the position reports on either side of the observation in question was determined and then divided by 12 hours.

It was found that the average translational speed for Eastern North Pacific tropical cyclones is 4.7 m s^{-1} . The average translational speed of Atlantic tropical cyclones is 6 m s^{-1} (DK1). The slower average storm speed for Eastern North Pacific tropical cyclones is probably not unexpected since Atlantic tropical cyclones are more likely to recurve poleward to a greater extent and get caught up in the westerlies (refer to Fig. 3).

After the translational speeds of each storm were subtracted from the record, several cases occurred in which the storm relative wind speed was negative. A negative storm relative wind indicates that the tropical cyclone was moving faster than the speed of the wind. The majority of these cases occurred over land and were subsequently eliminated. Negative storm relative winds occurring over the open ocean were found in hurricane Daniel (1978), tropical storm Carlos (1979), and tropical storm Miriam (1988).

Miriam became a tropical storm on 10/23/1988 but weakened considerably by 10/28/1800Z. Maximum winds at that time were reported at only 5 m s^{-1} with storm

relative winds ranging from -0.2 to -0.5 m s^{-1} . These conditions persisted for almost a two day period. Storm relative winds became positive again on 10/30/1200Z; however, Miriam never regained tropical storm strength. Thus, all observations in Miriam's record after 10/28/1200Z were deleted. The last observation in the records of Daniel and Carlos had storm relative winds of -0.7 m s^{-1} and -0.4 m s^{-1} respectively. These two cases were left alone since both storms were in their decaying stage and the reports were the last in each storm's record. Their inclusion does not affect the outcome of any results in this study.

3.2 Climatological SST Data

The next step in organizing the data base for this study was to assign a climatological SST to every observation in the adjusted Eastern Pacific best track data file. In order to remain consistent with the Atlantic study (DK1), the climatological SST fields used in this study were the result of the climatological SST analysis work of Levitus (1982). Levitus obtained SST data from the Oceanographic Station Data file and the Expendable and Mechanical Bathythermograph files maintained by the National Oceanographic Data Center. Levitus used computed potential temperature fields in place of the in situ temperature observations. The temperature and potential temperature are considered to be nearly identical in the upper 1000 m of the ocean (Levitus, 1982).

As described by DK1, monthly mean values of SST are assigned over a 1° by 1° latitude-longitude grid. The monthly mean SST values were linearly interpolated in time and space to the position and date of each tropical cyclone observation using the SST subroutine supplied by Dr. Mark DeMaria of the Hurricane Research Division. The climatological SST analyses are assumed to be valid in the middle of each month (DK1). Maps showing the monthly climatological mean SST in the Eastern North Pacific for the

15th day of each month from May through December are contained in appendix A. These maps were prepared from the grid mentioned above and compare well with other SST analyses (e.g., Newell *et al.*, 1972; Halpert and Ropelewski, 1989).

According to DeMaria (personal communication, 1994), the use of climatological SSTs in place of actual SSTs does not appear to pose a significant problem. His experience in the Atlantic was that most of the SST anomalies at the observed tropical cyclone locations are less than 1°C . This appears to also be true in the Eastern North Pacific based on the SST standard deviation maps from Halpert and Ropelewski (1989). It is noted that even during El Nino years, the SST anomalies in the Eastern North Pacific where tropical cyclones typically form and move are generally less than 1°C (e.g., Gray, fig. 1, 1984; Rasmusson and Carpenter, figs. 19, 20, 21, 1982).

If no SST was available for a given latitude-longitude coordinate, a value of 999.999 was returned by the subroutine. All of these cases, except one, occurred when the associated tropical cyclone was over land. These cases were eventually eliminated by the distance to land program described below. The one exception was the last observation in the adjusted record of tropical storm Katrina (1967). The storm position was reported as 30.9N, 114.6W which appears to be very close to land in the northern part of the Gulf of California. This observation was eliminated from the record.

3.3 Elimination of Land Cases

The Eastern North Pacific best track data file contains the positions of all Eastern North Pacific tropical cyclones regardless of whether the storm was over land or water. Because this study is concerned with the relationship between tropical cyclone intensity and SST, all the observations which occurred over land were eliminated using a distance

to land subroutine supplied by the Hurricane Research Division. The subroutine calculates the distance from, and normal bearing to, the nearest coastline to the center of the tropical cyclone. The center of the tropical cyclone is represented by the latitude and longitude reported in the best track file, and the coastline is represented by connected segments of varying lengths which define the basic shape of the coast. The starting point of each segment is given as a latitude-longitude coordinate. The distance from the cyclone center to the nearest point on each coastal segment is computed. The smallest absolute value is accepted as the distance of the tropical cyclone center to the coastline. A negative value indicates the tropical cyclone is over land and that observation is eliminated from the record. A total of 179 observations were eliminated by this program.

3.4 Other Adjustments to the Database

Final adjustments to the best track file involved 30 observations from various tropical cyclones which had moved over land then back over the ocean, and sometimes back over land again. Just over half (17) of the 30 observations involved only the last one or two reports at the end of a storm's life. To exclude the possible influence of land on the intensity, the 17 observations were eliminated from the dataset. The remaining 13 observations came from tropical storms Bridgette (1971) and Paul (1982). These two storms had moved over land for a period of 12 to 18 hours before moving back out over the ocean for an extended period of time.

Bridgette was a tropical storm before it moved over land and decreased to less than tropical storm intensity. After 12 hours, Bridgette moved back out over the ocean where it remained for another 48 hours but never regained tropical storm intensity. Thus, the observations (8) associated with Bridgette's movement back out over the ocean were

deleted from the record. The observations that were over land were eliminated by the distance to land program. Paul, on the other hand, did not reach tropical storm strength before moving over land. Paul remained onshore for 18 hours before moving back over water and subsequently develop into a tropical storm. The observations (5) associated with Paul's initial development were eliminated since Paul did not reach tropical storm strength before making landfall.

In all, a total of 2,006 observations were eliminated from the Eastern North Pacific best track data file from 1963 to 1993. The majority of these observations (1,796) were located west of 140°W and only 210 observations were eliminated due to land influences. The final dataset consisted of 11,062 observations containing the positions, intensities, and associated climatological SST of 467 tropical cyclones. The lowest climatological SST in the dataset was 16.0°C (only 1 observation) and the highest SST was 29.8°C (only 1 observation). All of the 467 tropical cyclones reached at least tropical storm intensity (maximum winds $>17 \text{ m s}^{-1}$), while 252 of these, about 54%, reached hurricane intensity (maximum winds $>33 \text{ m s}^{-1}$). DK1 found that approximately 63% of Atlantic tropical cyclones during the period 1962 to 1992 reached hurricane intensity. Comparing the percentage of tropical cyclones reaching hurricane intensity in the two ocean basins offers the suspicion that tropical cyclones in the Eastern North Pacific basin may not come as close to their maximum potential intensity as storms in the Atlantic.

3.5 Climatological SST Versus Tropical Cyclone Intensity

To get an initial idea of how SST and tropical cyclone intensity are related in the Eastern North Pacific, a scatter diagram was plotted (Fig. 9) showing the intensity and associated SST of all 11,062 observations in the 467 storm dataset. The scatter diagram

Intensity vs SST (Eastern Pacific Basin 1963-1993)

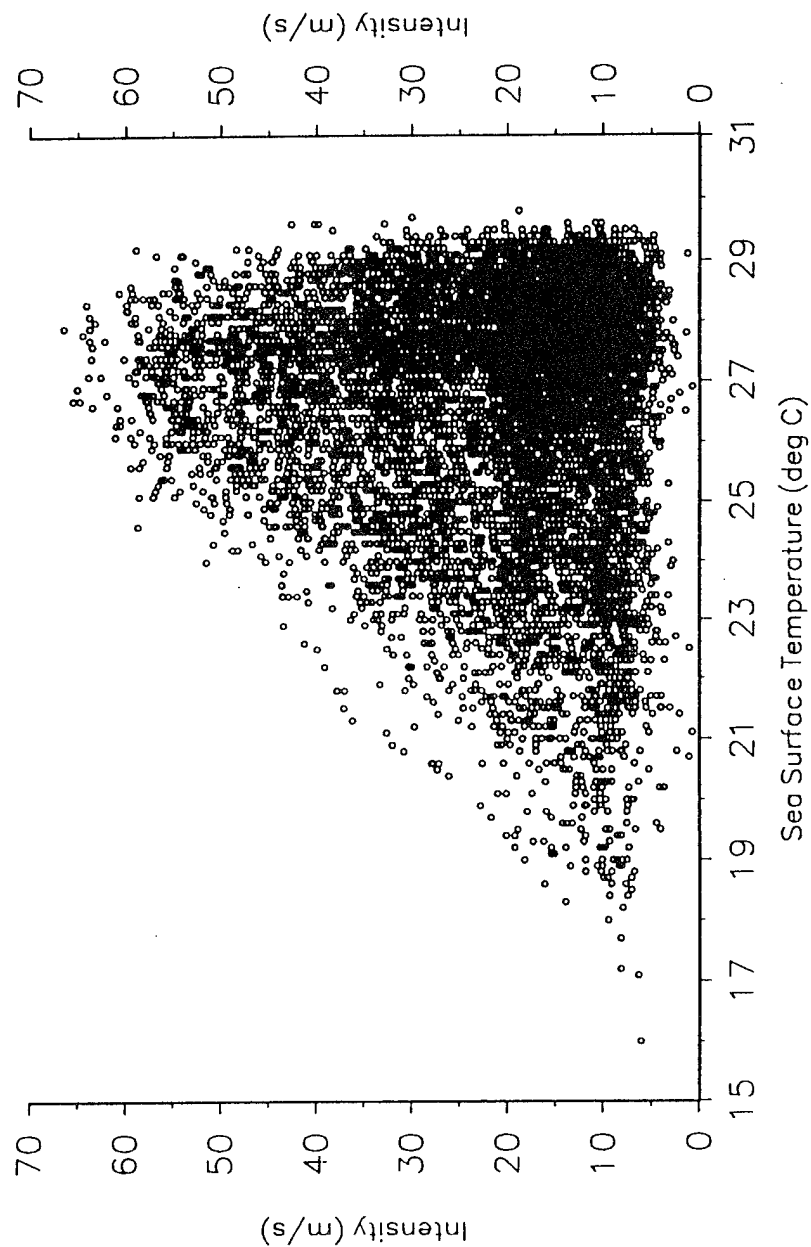


FIG. 9. Scatter diagram showing the intensity and SST of all 11,062 observations in the 31-year sample (1963-1993). Intensities are corrected for storm translational speed.

suggested a linear relationship between the maximum intensities and SST. Scatter diagrams from other SST/tropical cyclone intensity studies for other ocean basins (e.g., Merrill, 1985; Evans, 1993) do not indicate a linear relationship between SST and maximum tropical cyclone intensity.

The data were stratified by assigning each of the 11,062 observations to an SST group in the same manner as DK1. Eleven evenly spaced (1°C interval) SST groups were created ranging from 18.5° to 29.5°C. Properties of each SST group were determined and are shown in Table 1. Since only 9 observations were associated with SSTs <18.5°C (one at 16°C, two at 17°C, six at 18°C), these observations were combined with the 19°C SST group. This lowered the average SST for this group from 19.0°C to 18.8°C; however, this was not considered to be significant since the 19°C SST group represented less than one-half of one percent of the total observations.

TABLE 1. SST group properties.

SST Midpoint (°C)	Number of Observations	Avg SST (°C)	Avg Intensity (m/s)	Max Intensity (m/s)
19.0	52	18.8	10.8	20.1
20.0	58	20.0	11.7	26.1
21.0	141	21.0	14.6	36.2
22.0	282	22.0	14.5	39.1
23.0	472	23.0	16.5	43.5
24.0	700	24.0	19.2	51.5
25.0	923	25.0	23.1	58.7
26.0	1256	26.0	24.6	61.1
27.0	2042	27.0	23.7	65.5
28.0	3298	27.9	20.9	66.5
29.0	1838	28.8	19.3	60.7

Initially, a 30°C SST group (≥ 29.5 to $< 30.5^\circ\text{C}$) was also created which contained 31 observations with an average SST of only 29.5°C . Of the 31 observations, only one case was associated with an SST of 29.8°C , one case at 29.7°C , nine cases at 29.6°C , and the remaining 20 cases had SSTs equal to 29.5°C . Because the average SST was very close to the upper limit of the 29°C group, and to avoid having an SST group consisting of relatively few cases, these 31 observations were added to the 29°C SST group. The addition resulted in no change in the 29°C group's properties other than increasing the number of observations. An average SST of only 28.8°C for the 29°C SST group is probably a reflection of the very small area of Eastern North Pacific ocean covered by SSTs 29°C or higher (see appendix A). Eastern North Pacific tropical cyclones are not likely to remain over this very small region of 29°C ocean waters for very long; therefore, a smaller number of observations would be associated with SSTs 29°C or greater.

3.5.1 Intensity Curves

To determine how close storm observations come to their maximum intensity for a given SST, the maximum storm intensity along with the 99th, 95th, 90th, and 50th intensity percentiles for each group were determined. The maximum intensity for each SST group is shown in Table 1. Maximum intensities were found by searching each SST group for the maximum wind speed within that group.

The percentile intensities for each group are listed in Table 2. Percentile values of wind speed were found by placing the observations of each SST group in descending order (based on wind speed) and then determining the wind speed associated with the 99th, 95th, 90th, and 50th percent level for each group. The percentiles give an indication of the percentage of observations within an SST group that fall below the corresponding intensity. For example, the 50th percentile for the 29°C SST group indicates that the

TABLE 2. Intensity Percentiles

SST Group (°C)	99% (m/s)	95% (m/s)	90% (m/s)	50% (m/s)
19.0	19.2	18.2	16.2	9.5
20.0	22.8	21.0	18.9	10.9
21.0	32.6	27.3	21.4	13.8
22.0	37.0	27.9	24.6	13.0
23.0	40.8	32.8	28.0	15.3
24.0	44.8	36.8	32.9	17.9
25.0	54.3	44.9	41.2	19.8
26.0	57.2	51.6	46.6	20.4
27.0	58.1	52.4	45.1	19.3
28.0	56.3	48.1	40.2	17.4
29.0	54.2	41.7	35.0	16.6

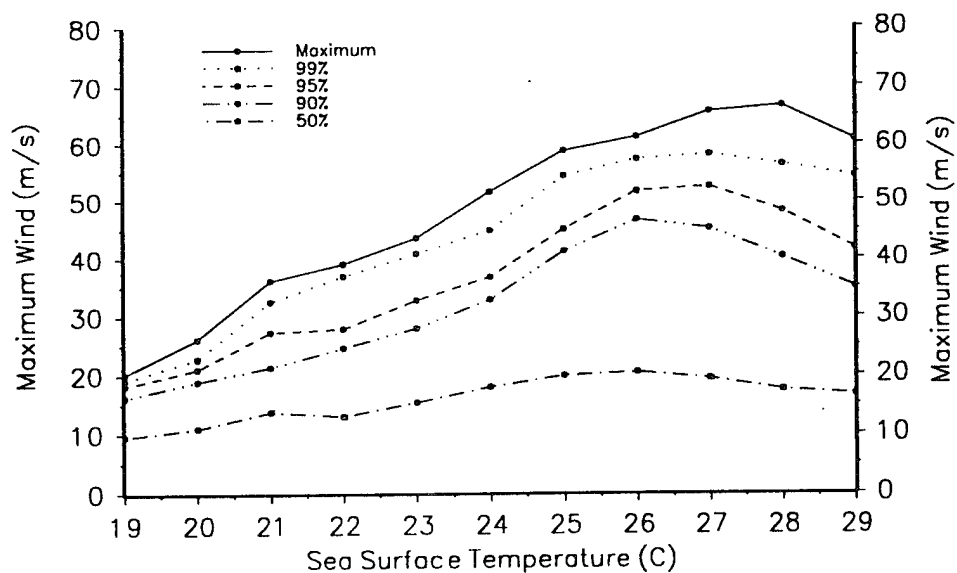
Intensity Curves for Eastern Pacific
(land cases removed)

FIG. 10. Intensity curves for the Eastern North Pacific with land cases removed and intensities corrected for storm translational speed.

TABLE 3. Eastern Pacific storms containing the maximum intensity data points.

SST Group (°C)	Storm Name	Year	Lat/Lon	Max Intensity (m/s)
19	Gwen	1972	28.9/120.2	20.1
20	Darby	1992	24.5/122.4	26.1
21	Darby	1992	23.4/119.0	36.2
22	Iselle	1990	23.4/119.2	39.1
23	Orlene	1992	21.0/135.5	43.5
24	Enrique	1979	19.6/130.7	51.5
25	Enrique	1979	18.9/129.9	58.7
26	Tina	1992	17.5/121.1	61.1
27	Hernan	1990	17.5/117.9	65.5
28	Trudy	1990	15.5/111.0	66.5
29	Ignacio	1979	17.0/107.3	60.7

intensity of 50% of the observations within the 29°C group do not reach tropical storm intensity (17 m s^{-1}). The remaining 50% of the observations are very close to (16.6 m s^{-1}) or above tropical storm intensity.

Intensity curves shown in figure 10 were prepared using the maximum and percentile intensity values. The maximum intensity curve implies a linear relationship between maximum intensity and SST over SSTs of 19 to 28°C. The decrease in intensities at SSTs of 28 to 29°C is thought to be a function of the small area of Eastern North Pacific ocean where these temperatures are found (refer to appendix A) and raises questions about the true relationship between the warmest SSTs and intensity. This idea will be discussed in the next chapter. The maximum intensity data points in figure 10 are used to develop an empirical maximum intensity relationship for Eastern North Pacific tropical cyclones. It is

noted that the maximum intensity data points come from only 9 storms in the dataset as shown in Table 3.

3.5.2 Development of the Empirical Maximum Intensity Function

DK1 smoothed their results by fitting an exponential function (eq. 3) to their maximum intensity observations using the method of least squares. Their choice of an exponential function was based on the shape of their maximum intensity and 99th percentile curves. In this study, the shape of the maximum intensity observations shown in both figure 9 and the shape of the maximum intensity curve in Fig. 10 (ignoring the 29°C SST group) suggested that a linear fit would be the most appropriate. An adaptation of the least squares curve-fitting program listed in James *et al.* (1985, pg. 337) was used to determine the best-fit line to the maximum intensity observations. The SST midpoints and the maximum intensity for each SST group were sent into the program and the program returned the constant coefficients of the given function (in this case a straight line). The program also calculated the correlation coefficient in order to determine the degree of association between SST and intensity as predicted by the function. The resulting equation represents the empirical maximum potential intensity relationship for Eastern North Pacific tropical cyclones and takes the form,

$$\text{EPMPI} = A + B(\text{SST}) \quad (4)$$

where EPMPI is the Eastern Pacific maximum potential intensity in units of m s^{-1} , SST is the sea surface temperature, and A and B are the constant coefficients determined from the least squares curve-fitting program.

The least squares curve-fitting program was run both with and without the 29°C SST group. The two lines that resulted were then compared to determine which was the better

fit to the maximum intensity data. A cubic spline was also fit to the maximum intensity data points. However, due to the uncertainty of the relationship between SST and intensity at the warmest SSTs, the cubic spline solution was not pursued further.

3.6 Comparison of Empirical Results With Theory

The Eastern North Pacific empirical results were then compared with the theoretical results of Emanuel (1988) following the method described in DK1 with the assumption that (4) is exactly satisfied. Maximum intensities (maximum winds) were computed from equation (4) and units converted from m s^{-1} to knots. The maximum winds were then related to sea-level pressures using the Dvorak (1984) empirical relationship between maximum wind speed and minimum sea-level pressure determined for the Atlantic (Table 4). The Atlantic maximum wind speed to pressure relationship was used since no such relationship has been investigated for Eastern North Pacific tropical cyclones. Also, the NHC uses the Dvorak Atlantic relationship when estimating intensities of Eastern North Pacific tropical cyclones from satellite data. Many, if not most, of the intensity estimates in the Eastern Pacific best track file since 1975 were made using the Dvorak technique. All of the maximum intensity data points, except one, used to create the EPMPI function came from storms after 1975 when the Dvorak technique was in use (see Table 3).

The entries in Table 4 with an asterisk are not part of the Dvorak empirical relationship. These entries were determined by continuing the trends in the maximum wind speed (MWS) and minimum sea-level pressure patterns seen in Table 4. For example, the amount of pressure change between current intensity (CI) numbers increases by one millibar for each increase in CI number. The change in MWS equals 15 knots over each of

TABLE 4. Dvorak empirical relationship between the current intensity number, the maximum wind speed (MWS), and the minimum sea-level pressure (MSLP) in tropical cyclones (Dvorak, 1984). Values with an * by them are not from the original Dvorak scheme. They are added here as described in the text and are used to help convert wind speeds predicted by the EPMPI equation to pressures.

Current Intensity Number	MWS (knots)	Atlantic MSLP (mb)	NW Pacific MSLP (mb)
1	25	####	####
1.5	25	####	####
2	30	1009	1000
2.5	35	1005	997
3	45	1000	991
3.5	55	994	984
4	65	987	976
4.5	77	979	966
5	90	970	954
5.5	102	960	941
6	115	948	927
6.5	127	935	914
7	140	921	898
7.5	155	906	879
8	170	890	858
###	*185	*873	####
###	*200	*855	####

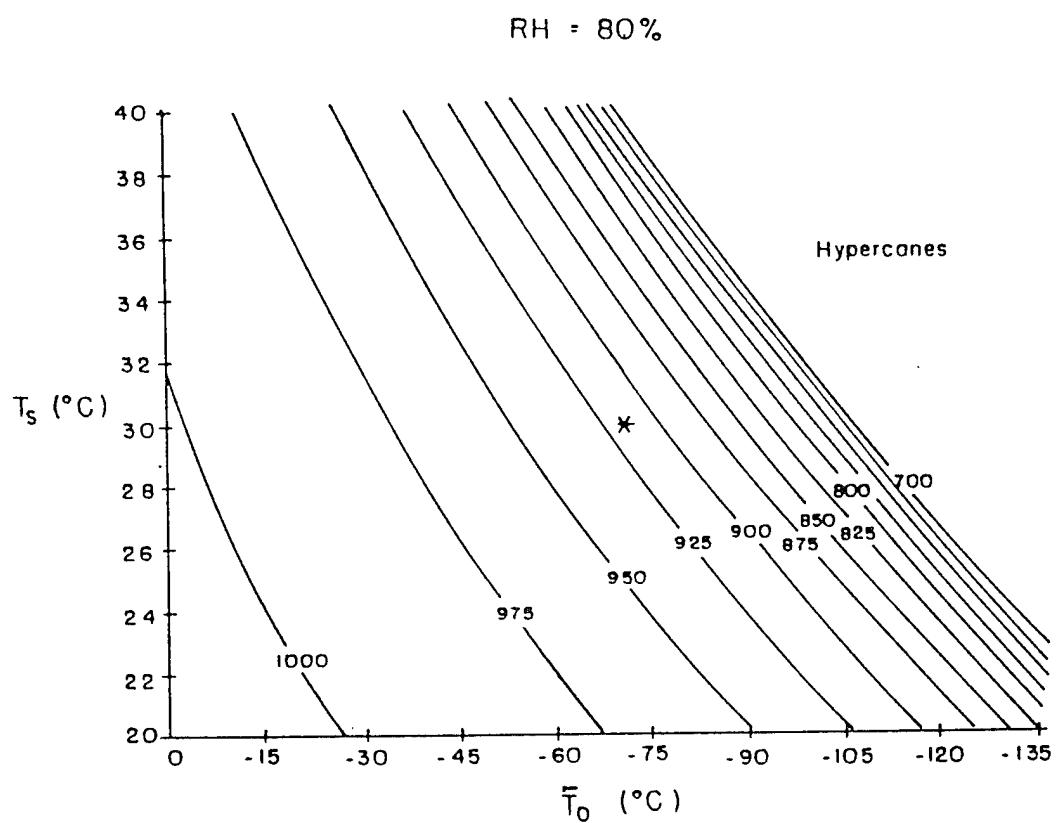


FIG. 11. Graphical representation of the minimum sustainable central pressure (mb) of tropical cyclones as a function of SST (T_s) and outflow temperature (T_o) assuming ambient surface relative humidity of 80% (Emanuel, 1988).

the last three CI numbers (7, 7.5, 8). Although these additional entries cannot be validated empirically, they do appear reasonable.

Using Fig. 11 (fig. 3a from Emanuel, 1988) and assuming an ambient relative humidity of 80%, the minimum sea-level pressure as determined above, and the associated SST were used to estimate the outflow temperature. The outflow temperature is considered to be the temperature at the top of the hurricane circulation and is generally found near the tropopause. The outflow temperatures were compared to climatological tropopause temperatures from Newell *et al.* (1972) to determine their reasonableness and to check the consistency between theoretical and observational results.

3.7 Relative Intensity

The intensity curves in Fig. 10 indicate that the majority of observations within each SST group fall far short of reaching their MPI. This suggests that most Eastern North Pacific tropical cyclones do not come close to their MPI. In DK1, the relative intensity was determined to obtain a clearer picture of just how close Atlantic tropical cyclones come to their MPI. The relative intensity is defined as the maximum intensity of the storm divided by its MPI as determined from (3) (DK1). Relative intensity is expressed as a percent. The same idea is applied in this study of Eastern North Pacific tropical cyclones.

For this study, the relative intensity is defined the same as in DK1. It is the maximum intensity in the storm record, minus the storm's translational speed, divided by the EPMPI determined from (4). Graphs showing the number of storms per 5% interval of relative intensity and the cumulative distribution of relative intensity are presented. Results are compared with those from DK1 to determine if Eastern North Pacific tropical cyclones come closer to their MPI than do Atlantic tropical cyclones.

DK1 further stratified the Atlantic dataset into 10° wide latitude (<20 , $20-30$, $30-40$, >40) bands and 20° wide longitude (<40 , $40-60$, $60-80$, >80) bands in order to aid in determining factors that may affect the relative intensity. The average relative intensity of storms falling within these bands was computed. Because Eastern North Pacific tropical cyclones do not exhibit as large a latitudinal or longitudinal variation as their Atlantic counterparts, the same stratification was not used here. Instead, storms were stratified into two latitudinal bands ($<18^\circ\text{N}$, $\geq 18^\circ\text{N}$) and two longitudinal bands ($<110^\circ\text{W}$, $\geq 110^\circ\text{W}$). The average relative intensities of storms falling on either side of these boundaries were then calculated.

The choice of 18°N and 110°W were selected to represent the dividing boundaries since the majority of storms appear to reach their maximum intensity south of 18°N and west of 110°W (see Fig. 12). The average latitude and longitude where tropical cyclones in the Eastern North Pacific reach their maximum intensity is 16.8°N , 115.1°W . Another reason for the above choice of coordinates is that a large portion of storms that form east of 110°W appear to have a tendency to remain east of 110°W and move northwestward along the coastline (e.g. Zehnder, 1993). Many of these storms end up moving north of 18°N . Zehnder (1993) also shows that storms forming west of 110°W are more likely to continue moving west or northwestward and remain south of 18°N . Figure 13 was taken from Zehnder (1993) and shows the initial formation points and movement of storms in the Eastern North Pacific from 1980 to 1989.

To determine how relative intensities change from month to month during the hurricane season, average relative intensities were computed for each month in which tropical cyclones were reported. Average relative intensities were also computed for each year in the 31-year dataset. The yearly averages were used to help determine how large-scale circulation features, such as El Niño and the stratospheric quasi-biennial oscillation (QBO), influence the innerannual variability in the average relative intensity of Eastern

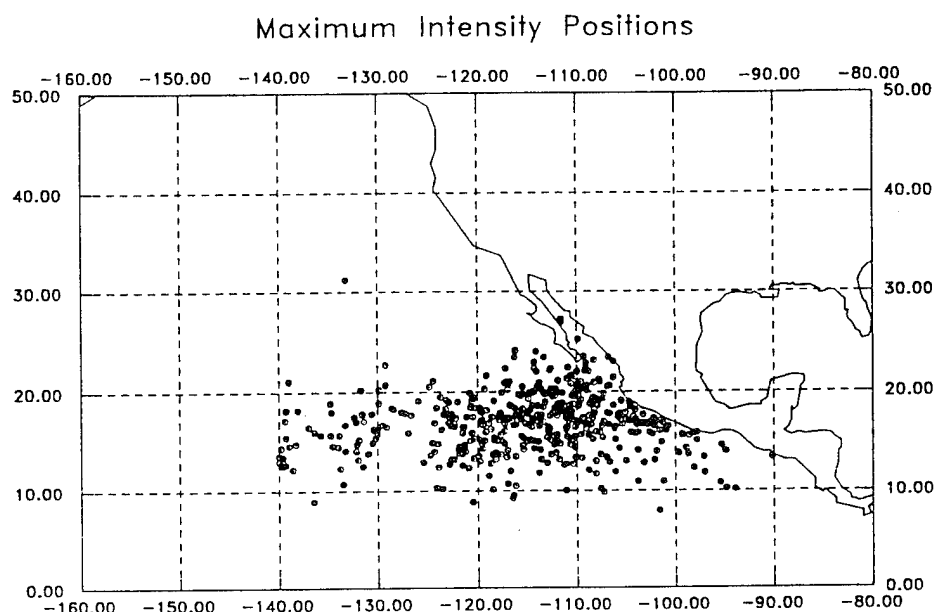


FIG. 12. Position of each of the 467 tropical cyclones in the 31-year sample at the time it reached its maximum intensity.

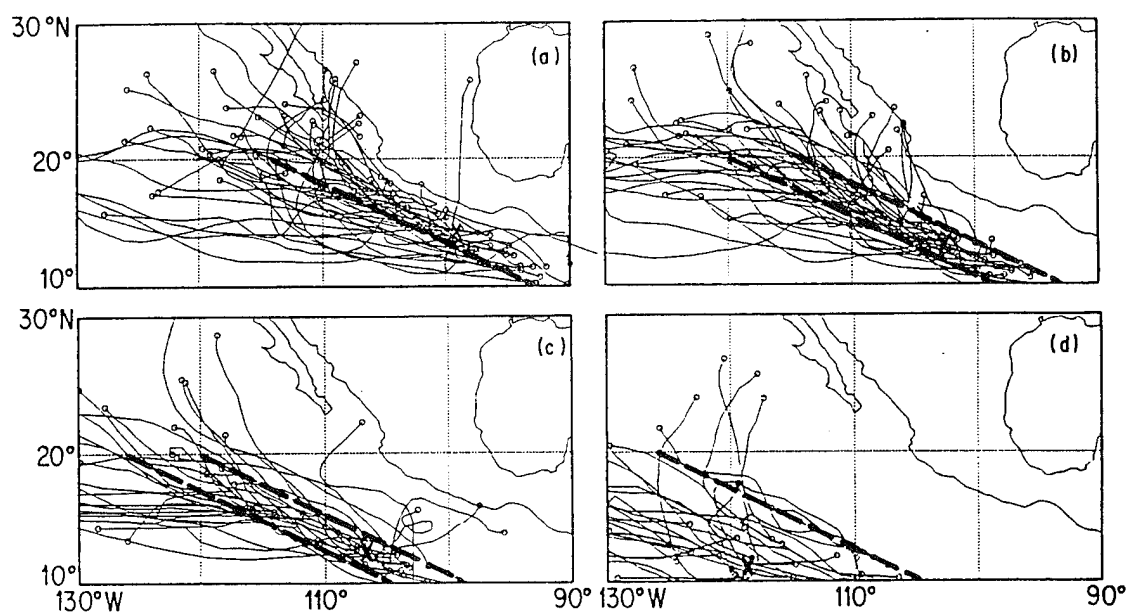


FIG. 13. Tracks of Eastern North Pacific tropical cyclones from 1980-1989. Cyclones originate east of the line in (a), between the lines in (b) and (c), and west of the line in (d). The symbol (X) marks the average initial location for each group (Zehnder, 1993).

North Pacific tropical cyclones. El Niño years used in this study are identical to those in DK1 (1965, 1972, 1976, 1982, 1983, 1986, and 1991). Only those years in which El Niño was considered to be of moderate or greater strength are counted as El Niño years. The year 1993 is considered to be a weak El Niño year. The average yearly relative intensities were also stratified using the phase (east, west, transition) of the QBO. With the exception of eliminating 1962 and adding 1993 as a west QBO year, QBO years were the same as those in DK1. It does not appear that El Niño or the QBO has much effect on the frequency of tropical cyclones in the Eastern North Pacific. This topic is discussed in more detail in the next chapter.

3.8 Required Cooling

In order to gain further awareness into whether tropical cyclone intensity is restricted by the SST, DK1 calculated the amount of cooling that would be required to increase the relative intensity of each storm, at its time of maximum intensity, to 100%. They (DK1) found that for their sample with land cases removed, the majority of storms (70%) required cooling of $>4^{\circ}\text{C}$ to obtain a relative intensity of 100%. DK1 suggested that this result indicated that tropical cyclone intensification is not limited by the SST. A similar analysis is accomplished for this study.

To determine the required cooling, a manipulation of equation (4) was used to calculate the SST using the observed maximum intensity reported in each storm record. The equation used was:

$$\text{SST} = (\text{EPMPI} - A)/B, \quad (5)$$

where EPMPI in this case is the actual maximum intensity and A and B are the same as in equation (4). The above SST is then subtracted from the actual SST to obtain the required cooling. The results are then plotted and compared with those for the Atlantic.

CHAPTER IV

ANALYSIS / RESULTS

4.1 Stratifying SST Data

Using whole degrees to represent the midpoints of the SST groups appears to provide a maximum intensity curve that fits the actual maximum data points reasonably well (Fig. 14). To check the sensitivity of the placement of the SST interval midpoint, SST groups ranging from 19 to 30°C were created using half degrees as the midpoint. Figure 15 shows the resulting maximum intensity curve plotted from these SST groups. Although this curve is not as smooth as the curve in Fig. 14, it does appear to outline the maximum intensity data points more closely.

The properties associated with the half-degree midpoint SST groups are shown in Table 5. Average SSTs for the lowest and highest SST groups in Table 5 are not as close to their midpoint as those in Table 1. The largest differences between the two curves occurs over the SST range of 22-25°C. The sharp increase in intensity at 24.5°C in the Fig. 15 curve is due to the shifting of a few higher intensity observations from the original 24°C and 25°C SST groups to the 24.5°C SST group. Centering the SST interval on the half degree shifts the maximum intensity data points of the warmest six SST groups towards colder temperatures by half a degree. For example, the maximum intensity data point at 28°C in Fig. 14 shifts to 27.5°C in Fig. 15 giving the appearance that the maximum intensities of Eastern North Pacific tropical cyclones do not occur over the

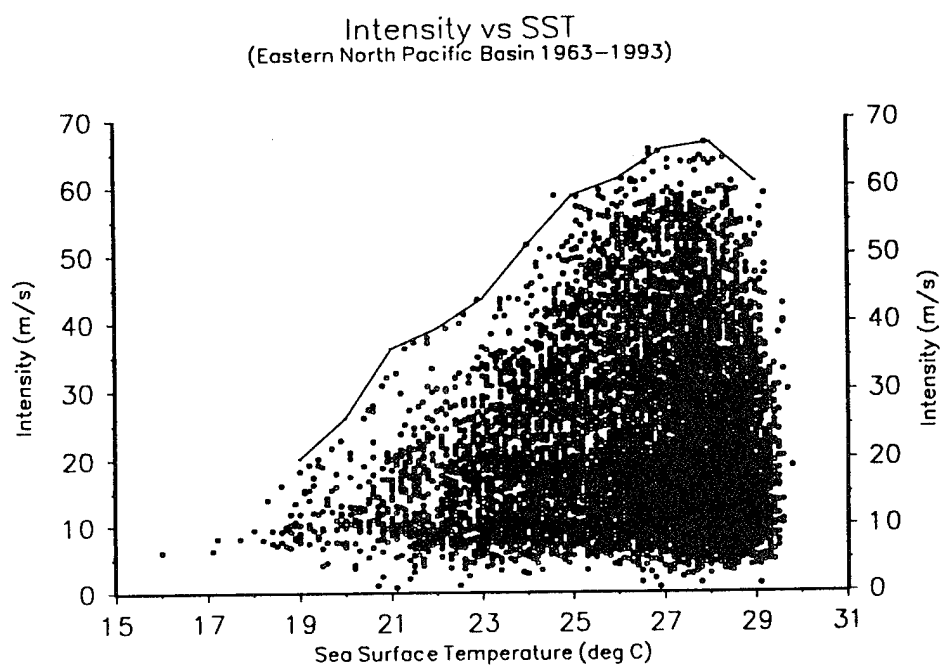


FIG. 14. Fit of maximum intensity curve to actual data using the SST groups in Table 1.

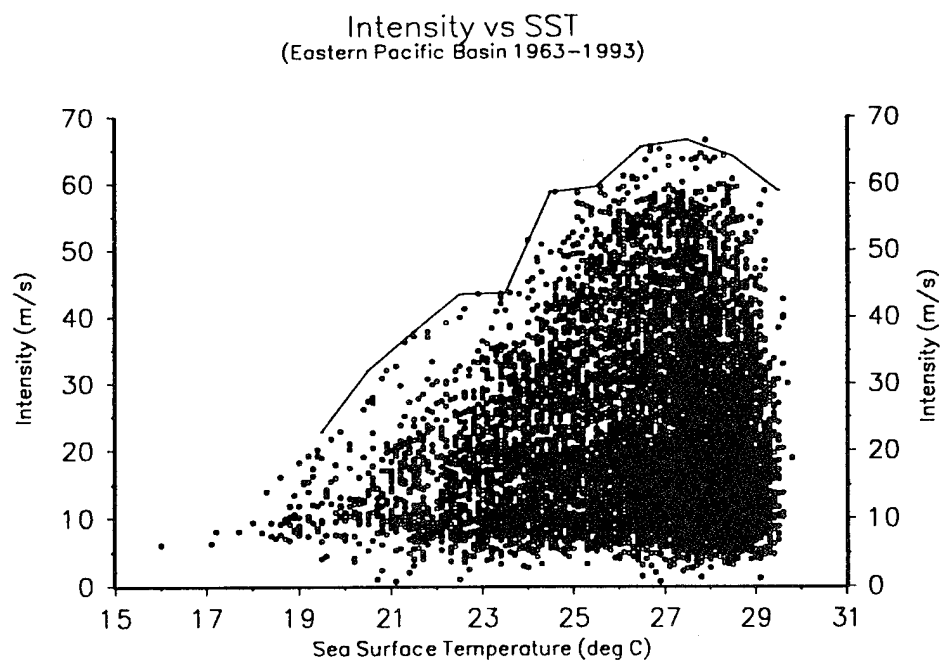


FIG. 15. Fit of maximum intensity curve to actual data using the SST groups in Table 5.

TABLE 5. Properties of SST groups when midpoints are placed at half degrees.

SST Midpoint (°C)	Number of Observations	Avg SST (°C)	Avg Intensity (m/s)	Max Intensity (m/s)
19.5	78	19.1	11.2	22.8
20.5	87	20.5	13.2	32.0
21.5	211	21.5	14.3	37.8
22.5	349	22.5	15.4	43.4
23.5	616	23.5	17.6	43.6
24.5	812	24.5	21.5	58.7
25.5	1012	25.5	23.9	59.5
26.5	1552	26.5	24.6	65.5
27.5	3026	27.5	22.4	66.5
28.5	2727	28.4	19.7	64.1
29.5	592	29.2	18.4	58.9

warmest waters. The climatological SST associated with this particular maximum data point is 27.9°C. The curve in figure 14 is accepted as the more representative of the relationship between SST and maximum intensity and is more in line with the theory that higher tropical cyclone intensities are associated with higher SSTs. The drop in intensity over SSTs of 28-29°C will be discussed in the next section.

The 26°C and higher SST groups (Table 1) comprised 76% of the observations in the 31-year dataset. This is less than the 82% found in the Atlantic study (DK1) for the 26°C-30°C SST groups. The smaller percentage of storms in the higher SST categories may simply be a function of the almost 4,000 more observations in the Eastern North Pacific dataset. It is suggested that this difference might also be due to the SST distribution and storm track patterns of the two ocean basins. Atlantic tropical cyclones move westward over increasingly warmer waters as they approach the Caribbean Sea and

the Southeastern U.S. before recurving poleward over colder waters. Eastern Pacific tropical cyclones, however, generally develop over the warmest waters and then travel west to northwest over colder ocean surfaces and, therefore, may spend less time over warmer waters than their Atlantic counterparts.

4.2 Intensity Curves

The percentile intensity curves in Fig. 10 appear to be well behaved in that they indicate a fairly steady rise in intensity up to SSTs of 26-27°C before levelling off and then dropping at 28-29°C. The maximum intensity curve increases steadily up to 28°C before decreasing at 29°C. Comparison of Fig. 12 with the climatological SST maps in appendix A clearly indicate that the majority of tropical cyclones in the Eastern North Pacific do not reach their observed maximum intensity over the area of 28-29°C SSTs. The average position where Eastern North Pacific tropical cyclones reach their maximum intensity is 16.8°N, 115.1°W, which is outside the region of 28-29°C climatological SSTs. The drop in intensities at SSTs of 28-29°C may be a result of tropical cyclones that initially develop over this region of warmest waters (e.g., Fig. 13) but move away over cooler sea surfaces before reaching their maturity.

Average intensities shown in Table 1 decline from the 26°C to 29°C SST groups. Since the majority of Eastern North Pacific tropical cyclones originate in the region where SSTs range from 27 to 29°C, the decrease in average intensities may be due to the lower intensities associated with initial development. To determine if this were true, the first 24 hour period of each storm's life was eliminated and the SST group properties recomputed. The results are shown in Table 6.

Only 14 of 1868 observations reported during initial development (first 24 hour period) of the 467 storms were associated with SSTs less than 26°C. The peak in average

TABLE 6. SST group properties with first 4 observations of each storm eliminated.

SST Midpoint (°C)	Number of Observations	Avg SST (°C)	Avg Intensity (m/s)	Max Intensity (m/s)
19.0	52	18.8	10.8	20.1
20.0	58	20.0	11.7	26.1
21.0	141	21.0	14.6	36.2
22.0	282	22.0	14.5	39.1
23.0	471	23.0	16.5	43.5
24.0	697	24.0	19.2	51.5
25.0	913	25.0	23.2	58.7
26.0	1227	26.0	24.8	61.1
27.0	1766	27.0	25.5	65.5
28.0	2400	27.9	24.2	66.5
29.0	1187	28.8	23.2	60.7

intensity shifted from the 26°C SST group (Table 1) to the 27°C group (Table 6) and the magnitude of the average intensity for the 27°C SST group increased by almost 2 m s⁻¹. The 28°C and 29°C groups showed the largest increase in average intensity, 3.3 and 3.9 m s⁻¹ respectively. These results lend support to the theory that higher intensities are associated with higher SSTs.

The decrease in average intensities at the 28°C and 29°C SST groups and the decline of the maximum intensity at 29°C is possibly due to storms that move away from the small area of 28 and 29°C ocean waters in the Eastern North Pacific before having a chance to reach a higher intensity. Negative influences from land may also hinder tropical cyclones from reaching higher intensities in the region of warmest waters, especially at SSTs of 29°C or greater. In the 31-year sample, roughly 84% of the observations associated with climatological SSTs $\geq 28.5^\circ\text{C}$ are within 500 km of land.

It is also possible that intensities of Eastern North Pacific tropical cyclones are often underestimated. Ships, instrumented buoys, and aircraft reconnaissance flights into the central region of tropical cyclones provide the most reliable measurements of central pressure and maximum winds. However, ship and buoy data are extremely limited and few tropical cyclones in the Eastern North Pacific are investigated by aircraft since the majority of them move away from land and do not pose a threat to life and property. This leaves satellite imagery as the primary means of estimating tropical cyclone intensity in the Eastern North Pacific. As mentioned previously, using the Dvorak satellite intensity prediction scheme developed for Atlantic tropical cyclones may produce less accurate results when used to estimate the intensity of Eastern North Pacific tropical cyclones. For the reasons discussed in the last three paragraphs, the decrease in intensity at the highest SSTs indicated by the intensity curves may not represent the true relationship between SST and maximum potential intensity of Eastern North Pacific tropical cyclones.

4.3 Empirical Maximum Potential Intensity Function

The maximum intensity curve in figure 10 was smoothed by fitting a linear function to the maximum intensity data points for the 19 through 28°C SST groups by the method of least squares. The 29°C SST group was ignored in the curve-fitting program because the decrease in the maximum intensity curve at those SSTs is not indicative of the common relationship between warmer water and stronger hurricanes. Equation (4), repeated here for clarity, represents the best-fit line to the maximum intensity data and is given by

$$\text{EPMPI} = A + B(\text{SST}). \quad (4)$$

EPMPI (m s^{-1}) represents the Eastern Pacific maximum potential intensity and SST ($^{\circ}\text{C}$) is the sea surface temperature. The constants determined by the least squares program are

$A = -79.17262 \text{ m s}^{-1}$ and $B = 5.361814 \text{ m s}^{-1} \text{ }^{\circ}\text{C}^{-1}$. Figure 16 shows the maximum intensity data with the EPMPI function. The average difference between the maximum intensity data points and the fitted function for SST groups 19-28°C is 2.0 m s^{-1} and the least-square error is 58.1. The correlation coefficient for the data and function is .987.

DK1 cautioned that their empirical MPI equation for the Atlantic may not accurately represent the relationship of SST to intensity at SSTs $>30^{\circ}\text{C}$. A similar situation exists with the EPMPI equation at SSTs $\geq 28.5^{\circ}\text{C}$. The decrease in the intensity curves (Fig. 10) at the warmest SSTs may be related to factors previously mentioned. Due to the uncertainty in the relationship between SST and intensity at the highest SSTs, the EPMPI equation should not be used when SSTs are $\geq 28.5^{\circ}\text{C}$. It is also noted that equation (4) is not valid at SSTs less than 16°C since no SSTs in the dataset were below this value. The function would predict negative intensities for SSTs less than 15°C . Because only a very few observations (<10) were linked with SSTs less than 18.5°C , it is recommended that the EPMPI equation not be used for SSTs $<18.5^{\circ}\text{C}$.

A least-squares fit was also placed on the maximum intensity data with the 29°C SST group included. Figure 17 shows the best-fit lines with and without the 29°C SST group. The best-fit line with the 29°C SST group underestimates the maximum intensities to a greater degree than the EPMPI function over SSTs of 24 to 27°C . Comparison of Fig. 12 with the climatological SST maps (appendix A) indicate that many Eastern North Pacific tropical cyclones reach their maximum intensity over SSTs in the 24 to 27°C range. Therefore, the fitted line to the maximum intensity data with the 29°C SST group included would not be as reliable a predictor of potential intensity as the EPMPI function over the 24 to 27°C SST range. For the line with the 29°C SST group, the average difference between the data points and the fitted function is 3.8 m s^{-1} over the 19 to 29°C SST groups and 2.7 m s^{-1} over the 19 to 28°C SST groups. The least square error (224.4) is approximately four times larger than that for the EPMPI function (58.1). Inclusion of the

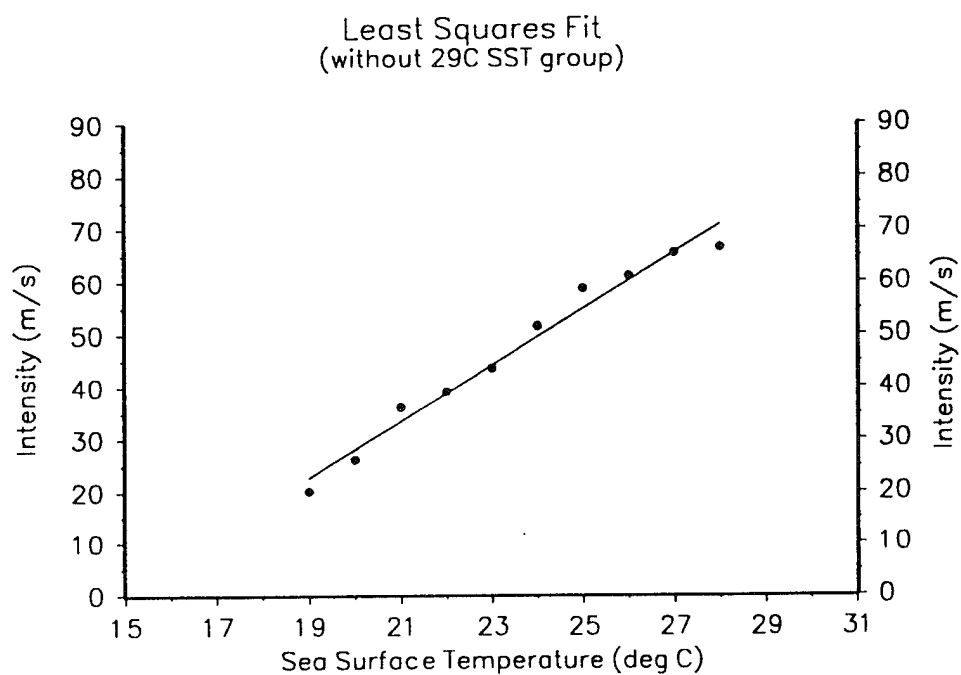


FIG. 16. The EPMPI function and the maximum intensity data from each SST group.

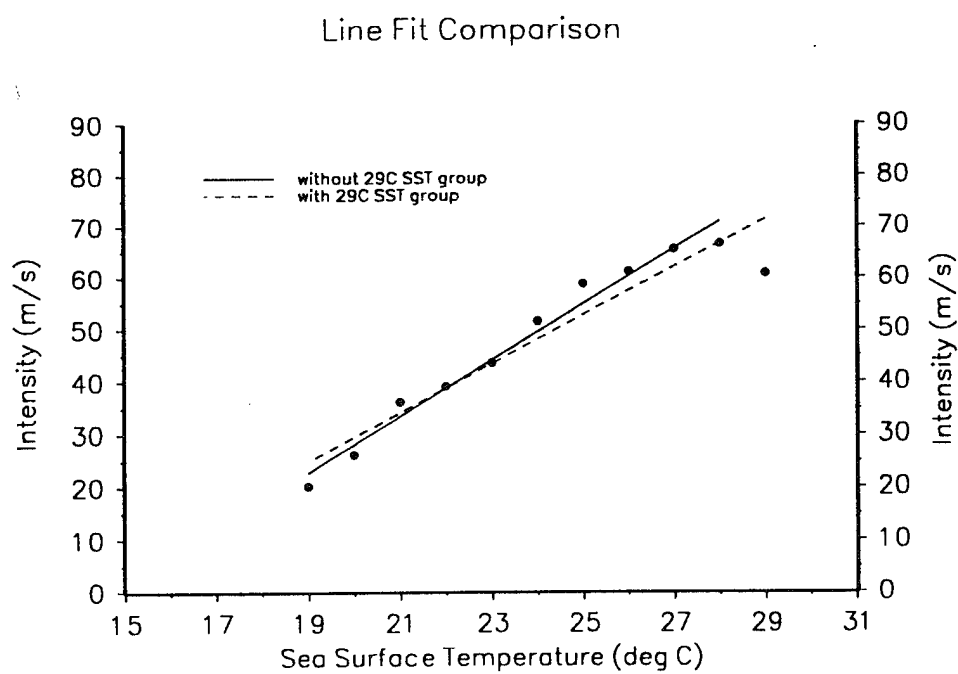


FIG. 17. Comparison of best-fit lines with and without the 29°C SST group and the maximum intensity data.

E. Pacific MPI vs Atlantic MPI

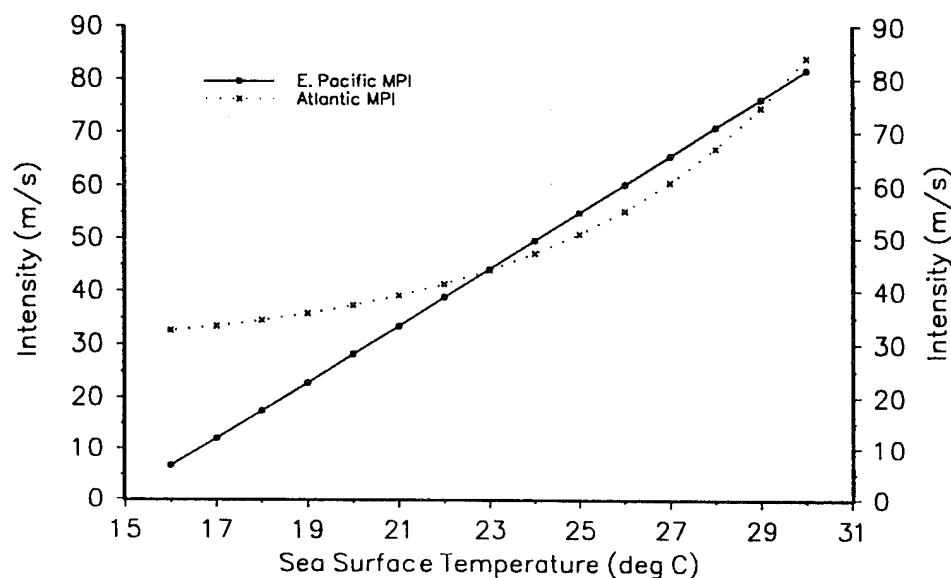


FIG. 18. Comparison between the Eastern North Pacific MPI and Atlantic MPI functions.

29°C SST group in the least-square fit does not address the uncertainty about the relationship between SST and maximum intensity at SSTs $\geq 28.5^{\circ}\text{C}$ and the function that results is not an improvement over equation (4).

Figure 18 compares the empirical maximum potential intensity functions for the Eastern North Pacific (eq. 4) and Atlantic (eq. 3) ocean basins. The two MPI curves are no more than 5 m s^{-1} apart from each other over SSTs in the 22–29°C range. A majority of tropical cyclones in both the Atlantic and Eastern North Pacific appear to reach their maximum intensities within the above range of SSTs. The departure between the MPI curves at SSTs less than 22°C is likely due, in part, to the greater number of fast moving Atlantic tropical cyclones that recurve poleward over colder waters and maintain a significant portion of their intensity. Positive interactions between the tropical cyclone and the environment (e.g., Molinari and Vollaro, 1989; DeMaria *et al.*, 1993) may also

contribute to the higher intensities observed in Atlantic tropical cyclones over colder waters.

4.3.1 Empirical Results versus Theory

Emanuel (1988) derived an expression that predicts the minimum central pressure (maximum intensity) of tropical cyclones as a function of SST, outflow temperature, and ambient relative humidity. DK1 used output from their Atlantic MPI function (eq. 3) to determine if the theoretical results of Emanuel (1988) were consistent with observed maximum intensities found in Atlantic tropical cyclones. Using the maximum intensities predicted by (3) (converted to pressure by the Dvorak relationship) along with the associated SST, DK1 found that the outflow temperatures determined from Emanuel's theory (Fig. 11) were compatible with climatological tropopause temperatures found above the tropical and mid-latitude Atlantic over SSTs of 24 to 30°C.

The current study uses the same analysis technique to compare equation (4) with the theoretical results of Emanuel (1988). Maximum intensities determined from equation (4) that did not convert directly to a Dvorak pressure value (Table 4) were assigned a pressure by computing the amount of pressure change per unit of wind speed between the appropriate Dvorak values and then interpolating. DK1 admits that the use of the Dvorak pressure-wind relationship will not produce completely accurate results. Because the Dvorak scheme for the Atlantic was based on data from Atlantic tropical cyclones, it's application to Eastern North Pacific tropical cyclones enhances the uncertainty of the intensity estimates.

Table 7 lists the outflow temperatures determined from Emanuel's theory (Fig. 11) along with the associated SST, maximum intensity, and surface pressure values. Outflow temperatures are plotted against SST in Fig. 19. Figure 19 shows the outflow temperature

TABLE 7. Relationship between the EPMPI function and outflow temperature based on the theory of Emanuel (1988). Minimum sea-level pressures (MSLP) from Dvorak (1984) have been interpolated where necessary.

SST (°C)	Maximum Intensity (from EPMPI)		Dvorak MSLP (mb)	Emanuel Outflow Temp (°C)
	(m/s)	(knots)		
19	22.7	45	1000	-35
20	28.1	55	994	-35
21	33.4	65	987	-43
22	38.8	76	979	-53
23	44.1	87	972	-60
24	49.5	97	964	-65
25	54.9	108	954	-67
26	60.2	118	945	-70
27	65.6	129	933	-74
28	71.0	139	922	-76
29	76.3	150	911	-77
30	81.7	160	901	-77
31	87.0	171	890	-77
32	92.4	181	878	-76

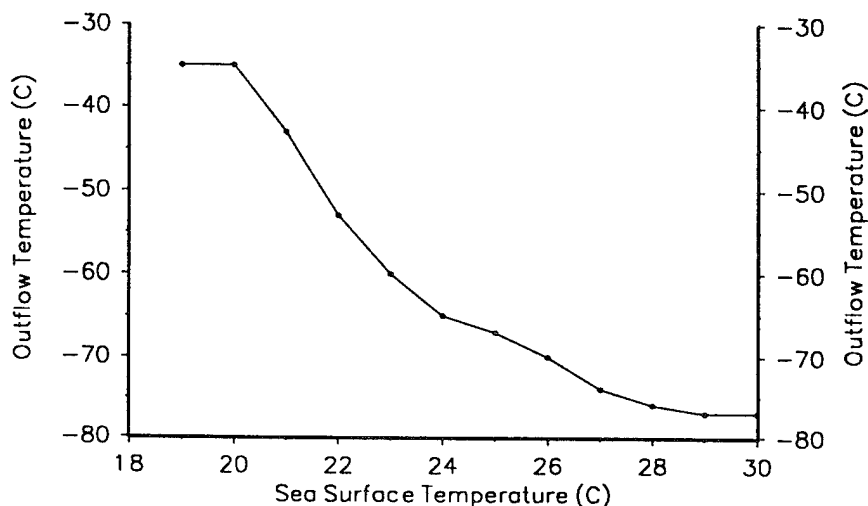


FIG. 19. The required outflow temperature as a function of SST needed to make the theoretical maximum intensity equal to the empirical maximum potential intensity for Eastern North Pacific tropical cyclones.

decreases gradually from -65 to -76°C as SST increases from 24 to 28°C . Climatological tropopause temperatures over the Eastern North Pacific ocean vary between -77°C near the equator to -68°C around 30°N during the hurricane season (Newell *et al.*, 1972). Thus, the outflow temperatures from -65°C to -76°C over SSTs of 24 to 28°C appear reasonable. This SST range includes 91% of the observations in the sample and covers the area over which a majority of Eastern North Pacific tropical cyclones reach their maximum intensity. According to DK1, the agreement between outflow and tropopause temperature indicates that Emanuel's (1988) theoretical results are consistent with the observations of maximum intensity.

The outflow temperatures over SSTs of 19 to 23°C decreased from -35 to -60°C . These outflow temperatures are more in line with upper-air temperatures found between

the 150 to 300 mb levels from 20 to 40°N latitude (e.g., Newell *et al.*, 1972) where SSTs in the 19 to 23°C range are found. The majority of tropical cyclone observations associated with SSTs in this range are of less than tropical storm strength (Table 2).

Outflow temperatures were also determined for SSTs greater than 28°C under the assumptions that the EPMPI function is valid at the higher temperatures and the additional pressure-wind relationship values to the Dvorak scheme (Table 4) are reasonable. Figure 19 and Table 7 indicate that the outflow temperature bottoms out and remains at typical climatological tropopause temperatures of -76 to -77°C as SSTs increase above 28°C. This is an interesting result because it appears to support the suggestion by DK1 that the tropopause temperature may be less sensitive to SST variations at SSTs above 29°C. It is also noted that the magnitude of the pressure decreases seen in Table 7 at SSTs $\geq 24^\circ\text{C}$ are in general agreement with equation (2) taken from Palmén and Newton (1969).

4.4 The Relative Intensity of Eastern North Pacific Tropical Cyclones

As mentioned previously, the majority of Eastern North Pacific tropical cyclones in the 31-year sample do not come very close to their MPI. The same was found to be true for DK1's sample of Atlantic tropical cyclones. DK1 suggested that the response of the ocean to the tropical cyclone circulation and unfavorable synoptic conditions such as vertical shear of the horizontal wind might be important factors that keep a storm from reaching its MPI. DeMaria (personal communication, 1994) speculated that Eastern North Pacific storms may come closer to their MPI than Atlantic storms. To determine if this is true, and to see how close Eastern North Pacific tropical cyclones come to their MPI, the relative intensity of each storm was calculated at the time it reached its maximum intensity.

The positions where each of the 467 storms reached their maximum intensity was shown in Fig. 12. Because the dataset was cutoff at 140°W, the true position of maximum intensity for some of the storms may have actually occurred west of this longitude. Very few storms in the sample reached their maximum intensity at positions north of 20°N and west of 120°W. SSTs poleward of 20°N are typically less than 24°C. The effect of the cooler ocean waters on the tropical cyclone circulation might be one reason few storms reach their maximum intensity over this region of the Eastern North Pacific. Evaporation may decrease due to the cooler SSTs and result in a decrease in the amount of energy available to the tropical cyclone, leading to a reduction in intensity. Vertical shear of the horizontal wind may also be a hindrance to tropical cyclone intensification in this part of the Pacific ocean. Analysis of the mean zonal (westerly) wind component (e.g., Newell *et al.*, 1972) and mean 200 mb streamlines/isotachs (Sadler, 1975) clearly indicate that the strength of the westerlies, and therefore the vertical wind shear, increases poleward of 20°N and westward of 120°W in the Eastern Pacific. Elsberry states that the few Eastern North Pacific tropical cyclones that do recurve poleward of 20°N have a tendency to decrease in intensity due to the low SSTs and the large vertical wind shear in this region (Elsberry *et al.*, 1987). It is also possible that large amounts of subsidence associated with the southeast quadrant of the Pacific High impedes tropical cyclone intensification in this region of the Eastern North Pacific.

Figure 20 shows the distribution of relative intensities for the 31-year sample broken down into 5% wide intervals of relative intensity. This figure verifies that very few Eastern North Pacific tropical cyclones reach their maximum potential intensity. The few cases that reached relative intensities greater than 100% were the result of the few storm observations that fell above the linear EPMPI function. The average relative intensity for the sample was only 49%. This is considerably lower than the 58% average relative intensity seen in Fig. 21 for the Atlantic sample with land cases removed (DK1). The

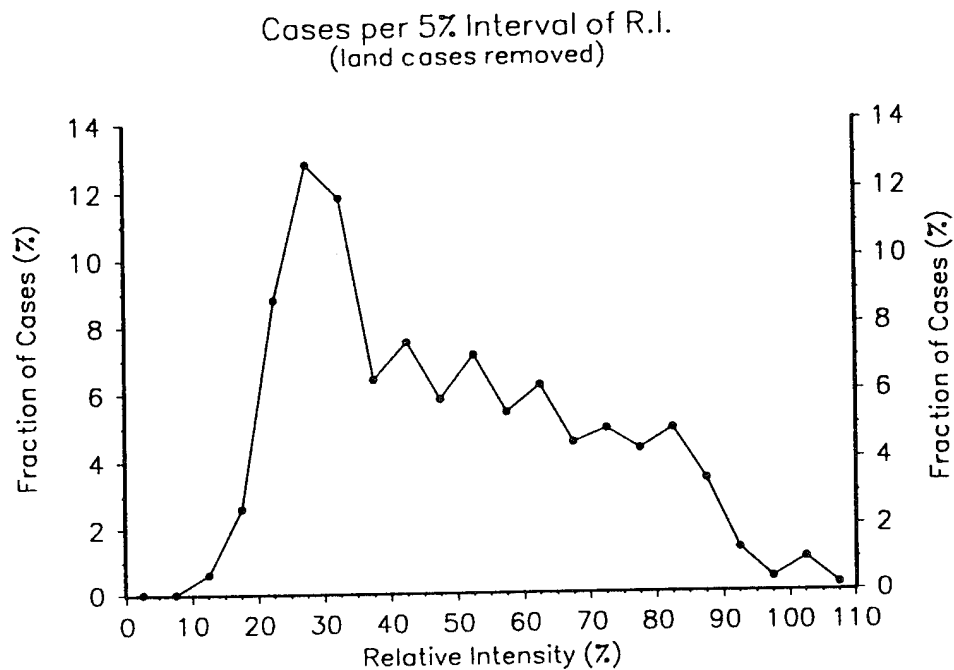


FIG. 20. The number of Eastern North Pacific tropical cyclones per 5% interval of relative intensity.

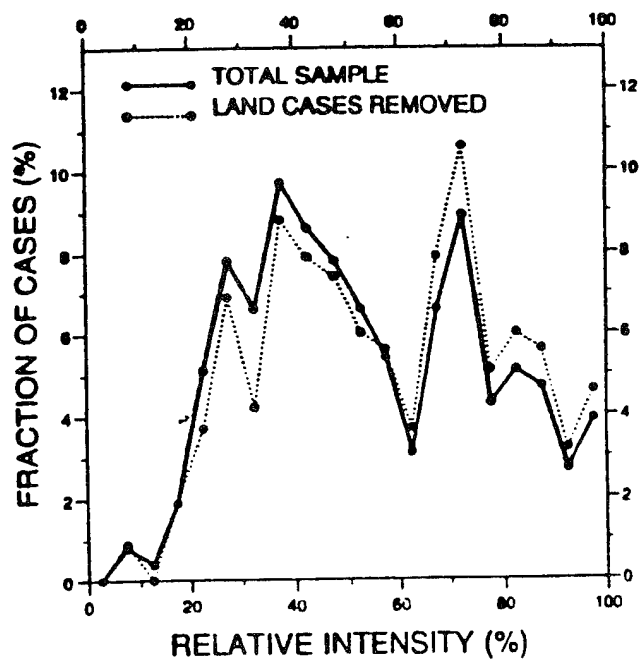


FIG. 21. Same as figure 20 except for the Atlantic (DK1).

difference in average relative intensities between the two ocean basins could be partly due to the larger number of Atlantic tropical cyclones that recurve poleward and have higher intensities at the colder SSTs. Because MPI decreases with decreasing SST, a high intensity storm over cold water will reach a greater portion of its MPI than a low intensity storm over water at the same temperature. It is also suggested that the ocean response to the tropical cyclone circulation may have a greater impact on the intensity of Eastern North Pacific storms than on Atlantic storms due to the differences in the thermal structure between the Eastern North Pacific (east of 140°W) and the Western Atlantic basins and because Eastern North Pacific storms generally have a slower translational speed. The ocean response is generally considered to be greater for slower moving storms (Bender, 1993; Schade, 1993; Price, 1981). The average translational speed of Eastern North Pacific tropical cyclones (4.7 m s^{-1}) is less than that for Atlantic tropical cyclones (6 m s^{-1}).

Figure 20 shows a peak in the distribution for relative intensities near 30% with a gradual decline over relative intensities from 40 to 85%. The distribution of relative intensities for the Atlantic (Fig. 21) from DK1 shows a bimodal structure with maxima near 40% and 70%. DK1 suggested that unfavorable synoptic conditions such as vertical wind shear might be important for storms that stop intensifying well before reaching their MPI and that the ocean response to the tropical cyclone circulation might be important to storms that stop intensifying after reaching a higher percentage of their MPI. The same argument could be applied to this study although the ocean response to the tropical cyclone circulation may play a larger role in Eastern North Pacific tropical cyclones.

Figure 22 shows the cumulative distribution of relative intensity for the 31-year sample of Eastern North Pacific tropical cyclones. Only 42-43% of the storms reached 50% of their MPI while only 11% reached 80% of their MPI. In the Atlantic sample with land cases removed, 58% of the storms reached 50% of their MPI and 19% reached 80% of

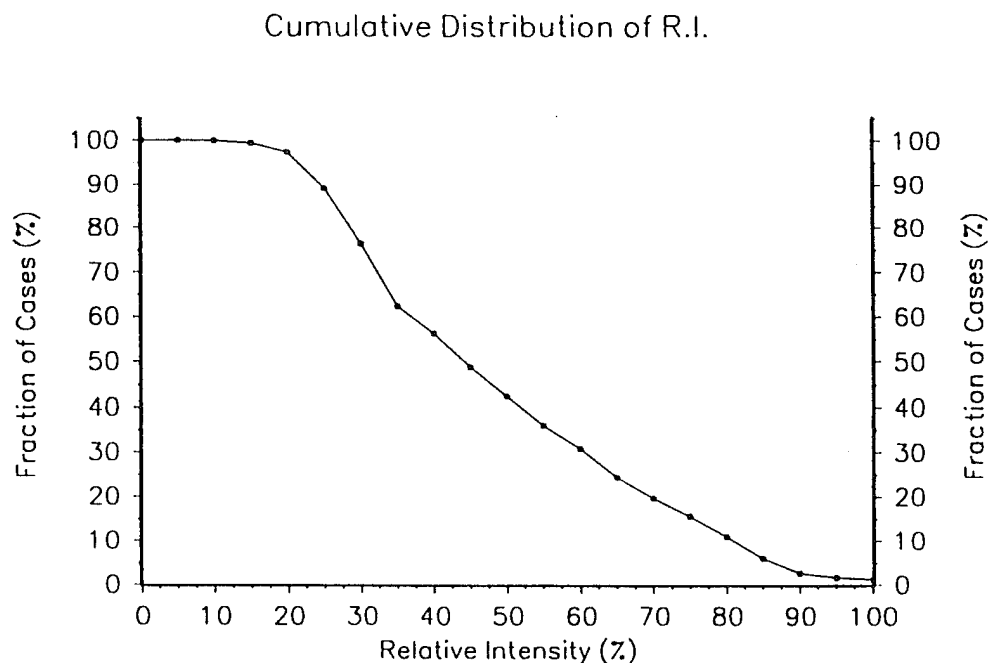


FIG. 22. Cumulative distribution of relative intensity (R.I.) for the Eastern North Pacific.

their MPI (DK1). These results do not support the speculation that Eastern North Pacific storms reach a much larger fraction of their MPI. Vertical shear of the horizontal wind, the response of the ocean to the tropical cyclone circulation, and subsidence associated with the Pacific High may all be factors contributing to the lower relative intensities. Another factor to consider is that if the intensities of Eastern North Pacific have generally been underestimated, then this error would be reflected in the relative intensities.

4.4.1 Distribution of Relative Intensity by Latitude/Longitude

To determine if the relative intensity of tropical cyclones varied by region in the Eastern North Pacific, the average relative intensities were calculated for storms north and south of 18°N and east and west of 110°W . The relative intensity of each storm was determined at the time it reached its maximum intensity before any averaging was done.

TABLE 8. Average relative intensity (R.I.) of Eastern Pacific tropical cyclones from 1963 to 1993 stratified by latitude and longitude.

Location		Number of Storms	Average R.I. (%)
Latitude (°N)	≥ 18	154	51.2
	< 18	313	47.5
Longitude (°W)	< 110	143	41.2
	≥ 110 to ≤ 140	324	52.0

The SST group properties for this stratification are shown in Tables 11-14 of appendix B.

Table 8 shows that the average relative intensity is slightly higher for tropical cyclones occurring north of 18°N. As suggested by DK1, the slight increase in average relative intensity with latitude could be due to storms that move north over colder water while still intensifying, thereby reaching a higher percentage of their MPI. The average relative intensity of Atlantic storms south of 20°N (50.5%) compares well with the values in Table 8 for the Eastern North Pacific. The overwhelming majority of tropical cyclones in the Eastern North Pacific reach their maximum intensity south of 20°N.

In Table 8, a marked increase is seen in the average relative intensity for tropical cyclones that reach their maximum intensity west of 110°W. Roughly two-thirds of the storms in the sample reached their maximum intensity west of 110°W. All but 14 of the tropical cyclone observations associated with climatological SSTs less than 27°C were positioned west of 110°W (Table 13, appendix B). This may partially explain the higher relative intensities in the region between 110°W to 140°W since tropical cyclones that are

still intensifying will attain a higher percentage of their MPI as they initially move over colder waters. Another reason for the higher average relative intensities is that the more intense storms occur in this region. Except for the 29°C SST group, the maximum intensity for each of the SST groups occurred in storms located west of 110°W. Many of the tropical cyclones that do reach their maximum intensity east of 110°W remain fairly close to land throughout their life. The influence of land on the tropical cyclone circulation may be one factor why storms east of 110°W do not attaining higher intensities and why lower average relative intensities are found in this region.

4.4.2 Stratification of Relative Intensity by Month

The average relative intensity for each month in which tropical cyclones were observed for the 31-year sample of Eastern North Pacific tropical cyclones is shown in Table 9. Tropical cyclone activity (number of storms) peaks during the months of July and August when the upper-level westerlies over the Eastern North Pacific are generally at their weakest. This is also the time when the area of 26 to 27°C SST water in the Eastern North Pacific appears to expand slightly and shift northward (appendix A). Allard (1984) noted a northward shift in the warmest waters of the Eastern North Pacific and in the ITCZ over the June to October period (Elsberry *et al.*, 1987). Based on the data from Levitus (1982), the area of SSTs 28°C and higher appears to shrink inward toward the coast as it extends northward into the Gulf of California from June through September (appendix A). It is possible that the frequent genesis of tropical cyclones in the region of highest SSTs causes a response in the ocean such that the top layer of warmest water is continually mixed with the cooler sub-surface water. This mixing may effectively cause the sea surface to become cooler and prevent the region of 28°C and higher SST waters to expand westward during the Eastern North Pacific hurricane season.

TABLE 9. Average relative intensity of Eastern North Pacific tropical cyclones stratified by month for the 31-year sample (1963 to 1993).

Month	Number of Storms	Average Maximum Intensity (m/s)	Average Relative Intensity (%)
May	11	29.5	42.0
June	61	30.3	46.0
July	112	30.4	48.0
August	110	30.8	48.7
September	95	34.3	52.5
October	68	33.6	49.4
November	9	26.7	38.6

It is notable that the peak month in tropical cyclone activity differs between the Eastern North Pacific and Atlantic ocean basins. In the Atlantic, the maximum number of tropical cyclones normally occur during the month of September when the SSTs in the western Atlantic are at their warmest and the area covered by the warmest SSTs is at a maximum. The drop in the number of tropical cyclones during September in the Eastern North Pacific could be related to changes in the large-scale circulation. Generally during September, the easterlies over the tropical and subtropical Atlantic begin to weaken (e.g., Newell *et al.*, 1972) while at the same time the westerlies are strengthening and shifting southward. Thus, fewer easterly waves may traverse Central America and spawn tropical cyclone formation in the Eastern North Pacific. The ITCZ also begins to shift back towards the equator during this time.

Table 9 indicates that the average relative intensity peaks in September but does not vary a great deal from July to October. Excluding November, average relative intensities

are lower during the early part of the hurricane season. In their sample of Atlantic tropical cyclones, DK1 also found that average relative intensities were lower in June-July and peaked in September. This result was considered surprising since the vertical wind shear over the tropical and subtropical Atlantic (and the Eastern North Pacific) is typically weakest during the June-July time frame (DK1). DK1 suggested that the lower average relative intensities for early-season storms could be a result of increased subsidence associated with the Bermuda-Azores High. The Bermuda-Azores High normally reaches its maximum pressure during July. A similar argument can be made to help explain why lower average relative intensities are found in Eastern North Pacific tropical cyclones during June-July since the Pacific High also reaches its maximum pressure in July. The sharp drop in average relative intensity in November may be due to the strengthening in the upper-level westerlies over the tropical and subtropical Eastern North Pacific.

4.4.3 Stratification of Relative Intensity by Year

DK1 found that there was considerable interannual variability in the average relative intensity for their 31-year Atlantic sample. Average relative intensities for their sample with land cases removed ranged from a low of 40.9% (1987) to a high of 74.4% (1992). Average relative intensity for each year of the Eastern North Pacific sample is shown in Fig. 23. Relative intensities range from a low of 32.6% in 1964 to a maximum of 63.7% in 1990. The low of 32.6% in 1964 may be somewhat questionable since it was computed from only 5 storms. Frank (Elsberry *et al.*, 1987) points out that prior to 1965, the number of tropical cyclones in the Eastern Pacific were significantly underestimated due to the lack of satellite imagery.

Figure 23 indicates that the average relative intensity of Eastern North Pacific tropical cyclones also varies considerably year to year. However, there appears to be a general

upward trend in the average relative intensity over the 31-year period. Average relative intensities were computed in 5-year increments for the 31-year sample and then plotted. The results (not shown) indicated a nearly linear increase in average relative intensity from a low of 41.2% (1963-1967) to a high of 55.3% (1988-1992). No such trend is evident in the 31-year sample of Atlantic tropical cyclones (DK1, Fig 8a., 1994). One explanation for this trend could be that with improved satellite imagery and analysis techniques, and as personnel gained experience in the use of these tools, intensity estimates also improved. The other possibility is that the trend of more intense tropical cyclones in the Eastern North Pacific is real. To examine this possible trend further, the average relative intensity curve shown in Fig. 23 was smoothed by applying an equally-weighted 5-year running mean statistical filter. Five-year running means were computed for the years 1965 to 1991 and then plotted in Fig. 24.

In Fig. 24, the large year to year fluctuations seen in Fig. 23 have been eliminated and a more explainable pattern has emerged. In the mid-1960's satellite imagery was still a recent technology and methods of determining tropical cyclone formation and intensifications from them were just beginning to be developed (e.g., Frett, 1966; Fritz, 1966). During the early 1970's the Dvorak scheme for estimating tropical cyclone intensity from satellite imagery was being tested and used in the field. Thus, it should not be too surprising that the average relative intensities seen in Fig. 24 increased from 1965 to 1973. From 1975 to 1987, the Dvorak scheme was the primary tool for estimating the intensity of Eastern North Pacific tropical cyclones. The 5-year running means (Fig. 24) indicate that intensity estimates were quite consistent during this time period. In 1988, the NHC took over responsibility for tropical cyclones in the Eastern North Pacific from the National Weather Service office in San Francisco. At this same time, average relative intensities began to increase (Fig. 24). Whether the increase in relative intensity since 1988 is related to procedures for estimating intensities at the NHC or to a "real" increase

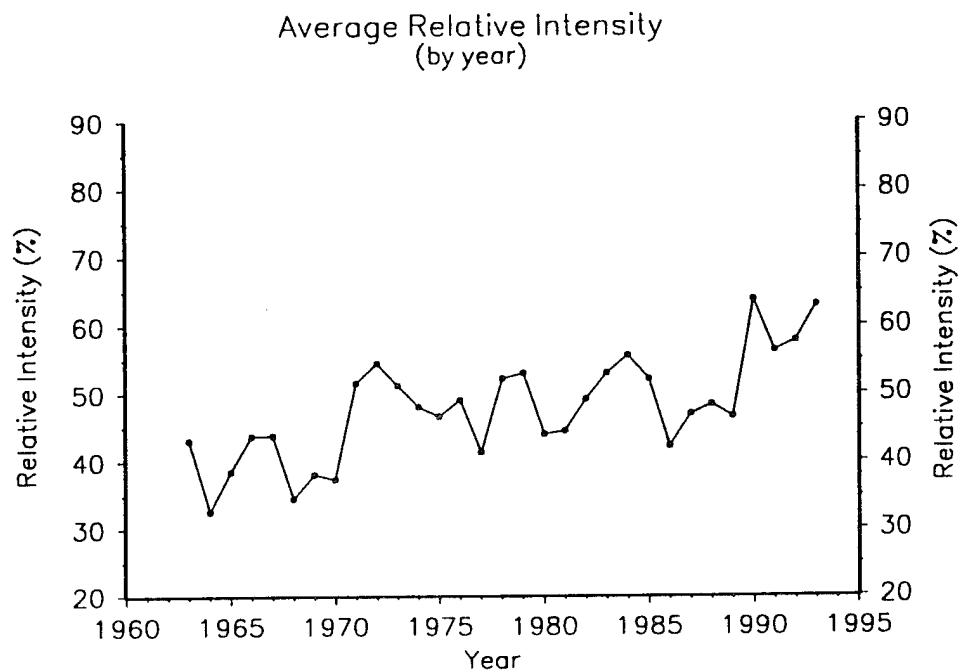


FIG. 23. Average relative intensities of Eastern North Pacific tropical cyclones for each year from 1963 to 1993.

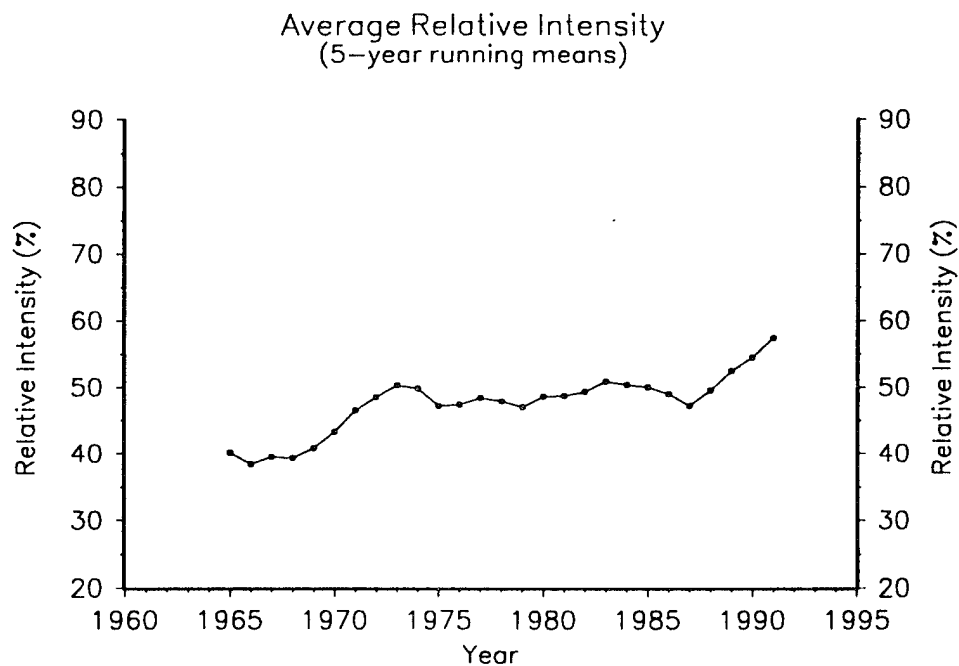


FIG. 24. 5-year running means of average relative intensity for the 31-year Eastern North Pacific sample (1963 to 1993).

in tropical cyclone intensities in the Eastern North Pacific is not known. It is also noted that 7 of the 11 maximum intensity data points from which the empirical function (4) was developed came from storms after 1989 (see Table 3) when the NHC had responsibility.

It is concluded that the general increase in average relative intensities seen in Figs. 23 and 24 up until 1988 is not the result of a "real" increase in the intensities of Eastern North Pacific tropical cyclones. Advancements in satellite imagery and interpretation methods, greater experience of personnel, and increased knowledge of tropical cyclone intensification processes are all likely explanations for the increase in average relative intensities over the period between 1963 to 1988.

4.5 Relationship of El Niño and the QBO to Eastern North Pacific Tropical Cyclones

Studies by Gray (1984) and Shapiro (1989) have contributed to establishing a relationship between the interannual variability of Atlantic tropical cyclone activity and large-scale circulation features such as El Niño and the QBO. DK1 found their results to be consistent with these studies. They found there are more tropical cyclones per season and the average annual maximum storm intensity is higher during years the QBO is in a westerly phase and in non-El Niño years. Gray (1984) has stated that El Niño events and the QBO has much less effect on the seasonal variability of tropical cyclones in the other ocean basins where tropical cyclones occur.

Table 10 shows the stratification of the Eastern North Pacific sample by El Niño events and the phase of the QBO. There appears to be very little difference in the frequency of Eastern North Pacific tropical cyclones (~15 per year) between El Niño and non-El Niño years or between east QBO and west QBO years, supporting Gray's assertion. However, other differences are noted. For example, during El Niño years, more storms reach their maximum intensity at positions farther west and slightly farther south than in non-El Niño

TABLE 10. Stratification of the Eastern North Pacific sample by El Niño and the phase of the QBO. El Niño years are the same as those in DK1. QBO years are the same as in Shapiro (1989), updated through 1992 by DK1. Entries in the 5 right-hand columns are based on the values when each storm reached its maximum intensity.

Factor	No. of Years	Avg # Storms per year	Avg Lat. (°N)	Avg Long. (°W)	Avg Max Intensity (m/s)	Avg MPI (m/s)	Avg R.I. (%)
El Niño	7	15.1	16.2	116.2	32.4	65.9	49.3
Non-El Niño	24	15.0	17.0	114.8	31.4	65.7	48.6
East QBO	13	15.0	16.8	114.5	30.4	66.0	46.6
West QBO	14	14.3	16.8	115.0	32.9	66.2	50.3

years. Gray (1984) noted that many tropical cyclones in the Northeast Pacific tend to track farther westward than normal during El Niño years. Some plausible explanations as to why this occurs are given below.

During El Niño years, the South Pacific trade winds are weaker than the North Pacific trade winds (Ramage and Hori, 1981) and the intertropical convergence zone (ITCZ) does not shift northward as far as normal. This may be one reason why storms reach their maximum intensity at positions farther south during El Niño years. A possible explanation for why tropical cyclones tend to reach their maximum intensity at positions farther west during El Niño years is seen in the analysis of 200 mb circulation patterns over the tropics and subtropics by Krishnamurti *et al.* (1982). Krishnamurti *et al.* (1982) prepared maps of 200 mb monthly mean streamlines for each year covering the period 1965 to 1974. Two major El Niño events occurred during this time period. The first was in 1965 and the

second in 1972. In the two El Niño years during the time of maximum tropical cyclone activity (August), the upper level anticyclone associated with the subtropical ridge over the Eastern North Pacific is centered farther to the west-southwest over the Eastern Pacific near 15° to 20°N and 120° to 140°W . In non-El Niño years, the analysis indicates that the upper level anticyclone is located either just offshore of Baja California or inland over the border of northern Mexico and the southwestern United States. The flow around the eastern side of the anticyclone may help keep storms farther south and west before they reach their maximum intensity.

The slightly higher average maximum intensities during El Niño years could be partially a result of enhanced outflow as storms move within the influence of the upper-level anticyclone just discussed. It is also noted that as tropical cyclones remain south of about 17°N during July to September, they generally remain over SSTs of 26 to 27°C . Ignoring the possible effects of the ocean response on the tropical cyclone circulation and unfavorable environmental factors, the longer the tropical cyclone remains over warm waters, the greater the likelihood the tropical cyclone will attain a higher intensity. Once storms move north of 18°N they encounter cooler waters which will have a negative impact on their intensity.

Table 10 shows that the average relative intensity and average maximum intensity of tropical cyclones in the Eastern North Pacific are higher when the QBO is in its west phase. The same was true for DK1's sample of Atlantic tropical cyclones. The higher average relative intensity indicates that tropical cyclones tend to come closer to their MPI in west QBO years. Both Gray (1984) and Shapiro (1989) have found that Atlantic tropical cyclone formation and intensification may be linked to the vertical wind shear conditions in the lower stratosphere (Gray *et al.*, 1993). Shapiro (1989) indicated that low-latitude Atlantic storms (south of 20°N) are more strongly related to the QBO than the seasonal total. Activity is inhibited during east QBO phases when vertical wind shear

in the lower stratosphere is enhanced. Gray *et al.* (1994) reports that recent studies (e.g., Knaff, 1993) indicate that tropical convection is favored near the equator (0° - 7° latitude) during QBO east phases and away from the equator (8° - 18° latitude) during QBO west phases. The majority of tropical cyclones in the Eastern North Pacific reach their maximum intensity at latitudes between 10° to 20° N. Since the QBO is a global feature, it seems reasonable to suggest that the vertical wind shear condition of the lower stratosphere might have some impact on the intensities of Eastern North Pacific tropical cyclones. More research is required to see if the above statement holds any weight. Statistical tests need to be applied to the results in tables 8, 9, and 10 to determine their significance.

4.6. Required Cooling

The temperature to which the SST must be cooled in order for the average relative intensity to reach 100% (required cooling) was determined for each storm at its time of maximum intensity as described in section 3.7.1. This was done to determine what effect SST might have on tropical cyclone intensification. Figure 25 shows the percentage of cases at 1° C increments of required cooling. No storm in the sample required an amount of cooling greater than 12° C. DK1 found that roughly 48% of the Atlantic storms in their sample with land cases removed required an amount of cooling in excess of 12° C.

Approximately 29% of the cases required cooling of 4° C or less (30% for Atlantic sample), 46% required cooling of 6° C or less (40% for Atlantic sample), and 71% required cooling of 8° C or less (46% for Atlantic sample). DK1 suggested that since the majority of cases required an amount of cooling $>4^{\circ}$ C, that Atlantic tropical cyclone intensification is not limited by the SST. As mentioned by DK1, the value of 4° C is the amount of cooling observed in the wake of Hurricane Gilbert by Shay *et al.* (1992).

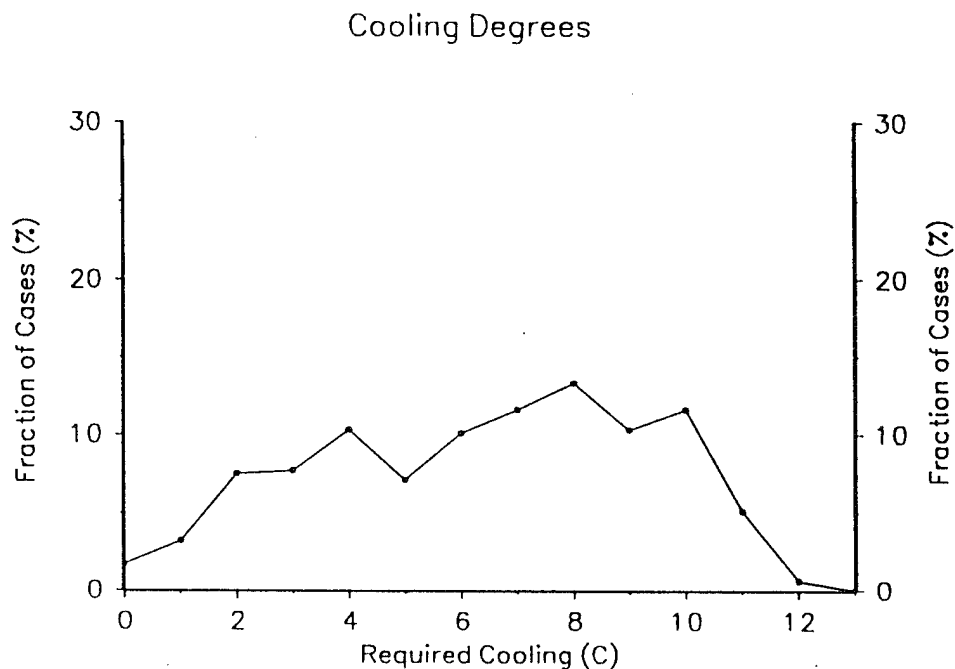


FIG. 25. Percentage of cases per 1°C increments of required cooling. Required cooling is the drop in SST needed to raise the average relative intensity to 100%.

However, other studies indicate the ocean response to the tropical cyclone circulation may result in a decrease in SST of as much as 6°C (e.g., Leipper, 1967; Price, 1981; Bender, 1993). Price (1981) concluded that the SST response depends heavily on 1) tropical cyclone strength, 2) storm translational speed, 3) the initial mixed layer depth, and 4) the temperature gradient of the upper thermocline. Differences in factors 2), 3), and 4) between the Eastern North Pacific and Atlantic basins might suggest that the effects of upwelling on storm intensity may be greater for Eastern North Pacific tropical cyclones than Atlantic tropical cyclones.

Eastern North Pacific tropical cyclones generally move slower than Atlantic tropical cyclones (4.7 m s^{-1} versus 6 m s^{-1}). The ocean response to the tropical cyclone circulation is expected to be greater for slower moving storms. Numerical results from Price (1981) indicated a decrease in SST of 4 to 5°C for storms moving at 4 m s^{-1} and a

decrease of 2 to 3°C for storms moving at 8.5 m s^{-1} . Based on the analysis of Levitus (1982), the depth of the mixed layer is shallower in the Eastern North Pacific where tropical cyclones reach their maximum intensity than in the Western Atlantic. There is some argument over the importance of the depth of the mixed layer on tropical cyclone intensity. Dr. Mark DeMaria (personal communication, 1994) of the HRD is of the opinion that the depth of the mixed layer is probably not that important since most storms are very far from their maximum possible intensity.

The temperature gradient is also much larger in the Eastern North Pacific with colder water nearer the surface. The thermocline in the tropical latitudes of the far Eastern North Pacific is very close to the surface and then increases in depth westward to roughly 150 m near 150°W (Philander, 1990). Given the slower storm movement, shallower mixed layer, and close proximity of the thermocline to the sea surface in the Eastern North Pacific, the ocean response to the tropical cyclone circulation may result in larger decreases in SST in the vicinity of the storm center of Eastern North Pacific tropical cyclones than of Atlantic tropical cyclones. Just how much of an impact a reduction in SST underneath a fairly localized region of a tropical cyclone can have on its intensity remains to be seen.

Numerical simulations of the interaction between the tropical cyclone and ocean by Bender (1993) indicate that a 5.6°C cooling of the SST induced by the tropical cyclone may decrease the intensity by 7 m s^{-1} for storms with no basic environmental flow. Cooling of 2.6 to 3.0°C in the SST and a decrease in intensity of 2.7 m s^{-1} resulted for storms with a basic environmental flow of 7.5 m s^{-1} . An observational network of buoys set up in the Eastern North Pacific in the area where tropical cyclones frequently track (e.g., Elsberry *et al.*, Fig. , 1987) could provide a significant amount of information on the magnitude of the ocean response and its impact on tropical cyclone intensity.

CHAPTER V

SUMMARY / CONCLUSIONS

The primary purpose of this work was to determine an empirical relationship between climatological SST and the maximum intensity of Eastern North Pacific tropical cyclones and to compare the results with those found for the Atlantic by DK1 and with the theoretical results of Emanuel (1988). A linear empirical relationship was developed from a 31-year sample of Eastern North Pacific tropical cyclones (1963-1993). This linear relationship (equation 4) represents an upper bound on the maximum intensity of Eastern North Pacific tropical cyclones located east of 140°W and is valid for SSTs in the 19 to 28°C range. Comparison of the intensity/SST scatter diagram in Fig. 6 with those of other ocean basins (e.g., Evans, 1993) suggests that the linear relationship is unique to the Eastern North Pacific.

This relationship was compared to the exponential relationship found for Atlantic tropical cyclones by DK1. The largest difference between the two functions comes from the large number of Atlantic storms that recurve poleward over cold waters less than 22°C. Over SSTs of 22 to 28°C, the two curves are within 5 m s^{-1} of each other. Uncertainties exist in both the Eastern North Pacific and Atlantic MPI functions at SSTs greater than 28°C and 29°C respectively. In the Eastern North Pacific, the area of 29°C SSTs is quite small and located close to the coast. Many storms in this area are undergoing development and may not have a chance to reach their maturity before moving over colder waters or onshore. This may explain the decrease in maximum intensity at

SSTs greater than 28°C.

The EPMPI function was also compared to the theoretical results of Emanuel (1988). Assuming the tropopause temperature is a function of SST, the outflow temperatures predicted from Emanuel's theory are consistent with climatological tropopause (100 mb) temperatures over the tropical Eastern North Pacific for SSTs $\geq 24^{\circ}\text{C}$. At SSTs below 24°C, predicted outflow temperatures compare with climatological temperatures found between 300 to 150 mb over the subtropical Eastern North Pacific.

Speculation that Eastern North Pacific tropical cyclones come much closer to their upper bound than storms in other basins is not supported. The observed maximum intensity of each storm was divided by its empirical maximum potential intensity, calculated from the EPMPI function, to determine its relative intensity. The cumulative distribution of relative intensity showed that only about 42% of tropical cyclones in the Eastern North Pacific reach 50% of their MPI and only 11% reach 80% of their MPI. These percentages are considerably lower than the 58% and 19% found for Atlantic tropical cyclones. The results do agree with other studies that very few tropical cyclones come very close to their MPI.

Why Eastern North Pacific tropical cyclones do not come as close to their MPI than storms in the Atlantic is not easily determined. Tropical cyclones in the Eastern North Pacific spend their lifetime over a fairly localized region and generally do not recurve poleward to high latitudes. Many Atlantic tropical cyclones, however, recurve poleward over cooler waters while maintaining a large portion of their intensity and thus reach a higher percentage of their MPI. Storms that do recurve poleward in the Eastern North Pacific generally encounter strong vertical wind shear. Differences in the thermal structure between the two ocean basins suggests that the ocean response to the tropical cyclone circulation may have greater significance for Eastern North Pacific tropical cyclones than those for the Atlantic. Other studies indicate that the negative effects of upwelling on the

storm circulation will be greater for slower moving tropical cyclones and over areas where the temperature gradient of the upper thermocline is large. Both of these conditions are found in the Eastern North Pacific. More studies are needed to determine just how large an impact upwelling can have on the tropical cyclone circulation for ocean conditions common to the Eastern Pacific.

Stratification of the 31-year sample by latitude, longitude, and month produced results similar to those of DK1. The average relative intensity was greater for storms north of 18°N and west of 110°W . The average relative intensity for Atlantic storms that reach their maximum intensity south of 20°N is comparable to the average relative intensities of Eastern North Pacific storms of which the majority reach their maximum intensity south of 20°N . This would seem to suggest that poleward recurving tropical cyclones over cooler waters is a major reason why Atlantic storms reach a higher portion of their MPI than storms in the Eastern Pacific. Results of the monthly stratification showed that tropical cyclones tend to reach a higher percentage of their MPI in August-October than during June-July. This result was also true of Atlantic tropical cyclones (DK1) and may be partly due to increased subsidence associated with the subtropical highs during July.

Stratification of average relative intensity by year showed that there is substantial interannual variability. Five-year running means of average relative intensity were determined to help explain the general upward trend in average relative intensity over the 31-year period. The two periods of increased intensity seen in Fig. 21 appear to correlate with 1) the development of the Dvorak intensity prediction scheme and 2) the time when the NHC took over responsibility of tropical cyclones in the Eastern Pacific. El Niño and the QBO appear to have almost no effect on the frequency of tropical cyclones. Average maximum intensity and average relative intensity are greater during El Niño and west QBO years than during non-El Niño and east QBO years. Eastern North Pacific tropical cyclones tend to reach their maximum intensity at positions slightly farther south and

farther west during years of El Niño. This feature may be related to changes in the upper-level circulation pattern over the Eastern North Pacific during El Niño years.

The amount of cooling required to increase the relative intensity of each storm at its time of maximum intensity to 100% (results in a decrease in MPI) was calculated to determine if storm intensification was limited by the SST. Results showed that the majority of storms (71%) required cooling of $>4^{\circ}\text{C}$ but $\leq 8^{\circ}\text{C}$ in order to raise the relative intensity to 100%. Decreases in SST induced by the tropical cyclone circulation to the magnitude of 8°C has not been demonstrated and is probably not likely to occur in the vicinity of a moving storm center where the cooling is needed. Recent studies indicate that cooling by as much as 6°C may be possible for slow moving storms. Thus, the ocean response to the tropical cyclone circulation on the storm intensity may be important in roughly half the cases (46%). This is a subject requiring further study.

The use of climatological SSTs and manually estimated intensities derived from satellite imagery certainly leaves room for improvement. DK1 suggested that SST analyses averaged over shorter time periods could refine the results. More accurate methods of determining intensity would also help. In situ measurements of intensity (wind speed, pressure) and actual SST would be ideal but probably not very cost effective.

Whether or not the EPMPI function is a closer representation of the true relationship between SST and maximum intensity than the Atlantic MPI function from DK1 is debatable. The Atlantic MPI function may suffer from more "noise" which obscures the actual relationship. The term "noise" refers to interactions between the tropical cyclone and the large-scale environment (i.e., upper-level troughs and cold lows) which cause storms to recurve poleward and maintain higher intensities over colder waters than storms in the Eastern North Pacific.

Finally, it is hoped that the EPMPI function developed for this thesis will be useful in improving future intensity estimates of Eastern North Pacific tropical cyclones. A

statistical hurricane intensity prediction scheme similar to DeMaria and Kaplan's (1994b) SHIPS model is currently being worked on for the Eastern North Pacific. The EPMPI function will be one small part of this prediction scheme.

APPENDIX A

MAPS OF MONTHLY CLIMATOLOGICAL SST FOR THE EASTERN NORTH PACIFIC OCEAN

MAY CLIMATOLOGICAL SST

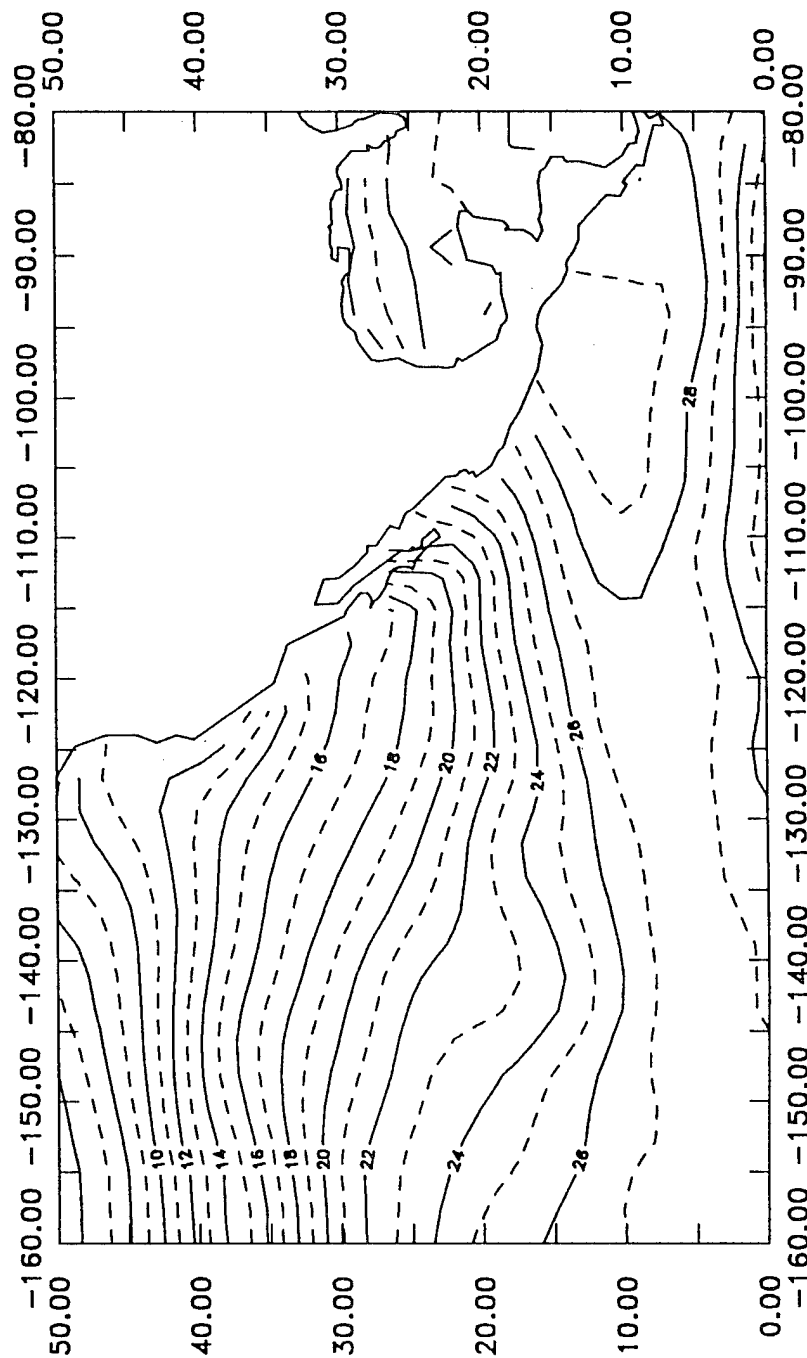


FIG. 26. Climatological sea surface temperatures for the month of May.

JUNE CLIMATOLOGICAL SST

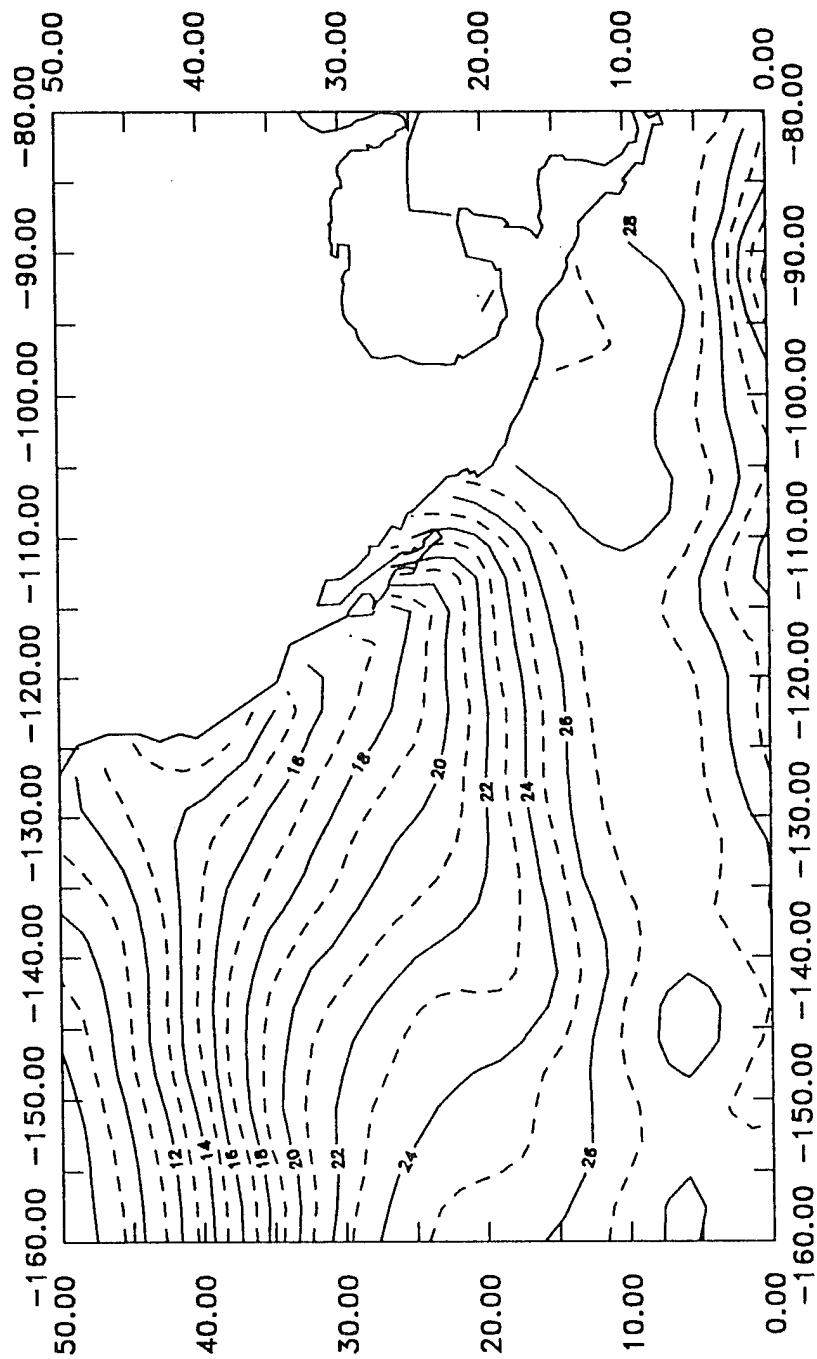


FIG. 27. Climatological sea surface temperatures for the month of June.

JULY CLIMATOLOGICAL SST

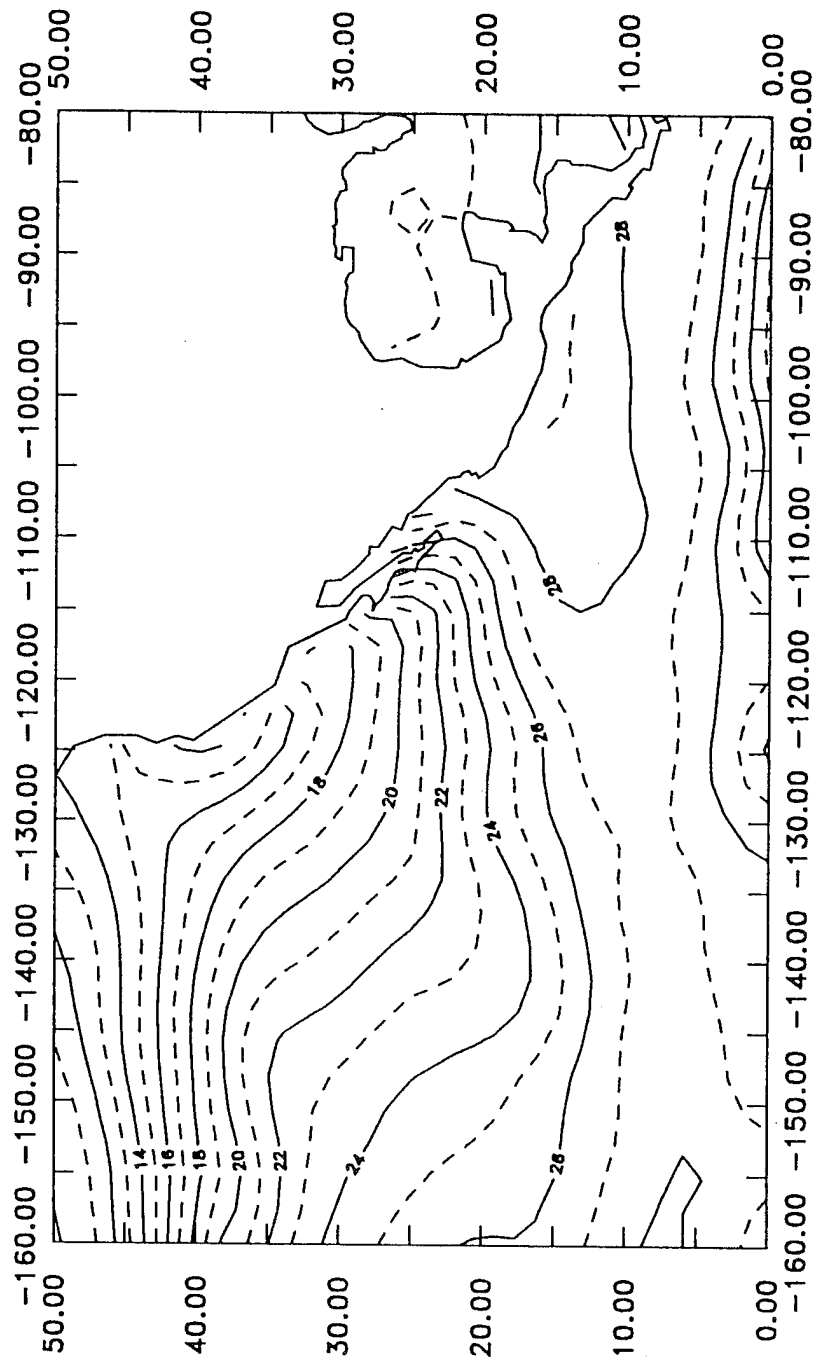


FIG. 28. Climatological sea surface temperatures for the month of July.

AUGUST CLIMATOLOGICAL SST

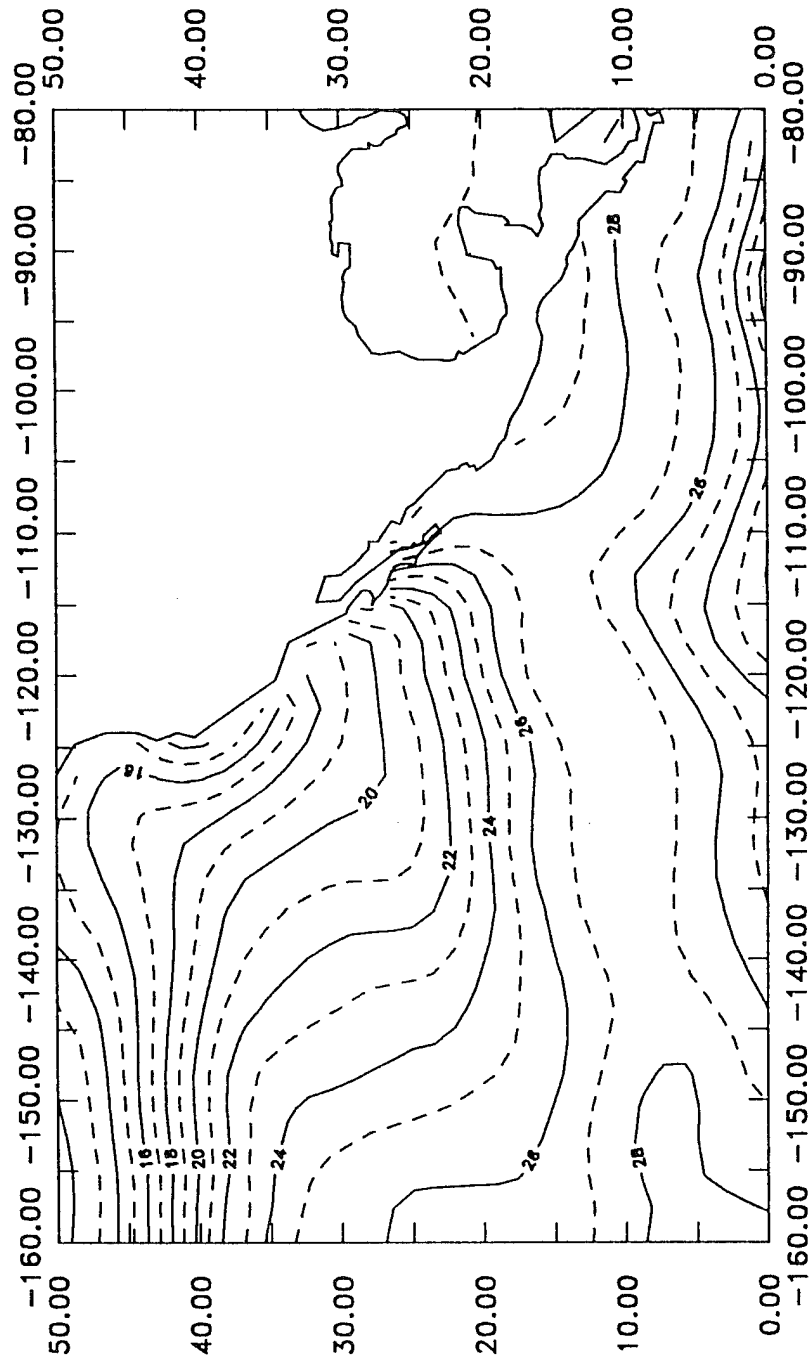


FIG. 29. Climatological sea surface temperatures for the month of August.

SEPTEMBER CLIMATOLOGICAL SST

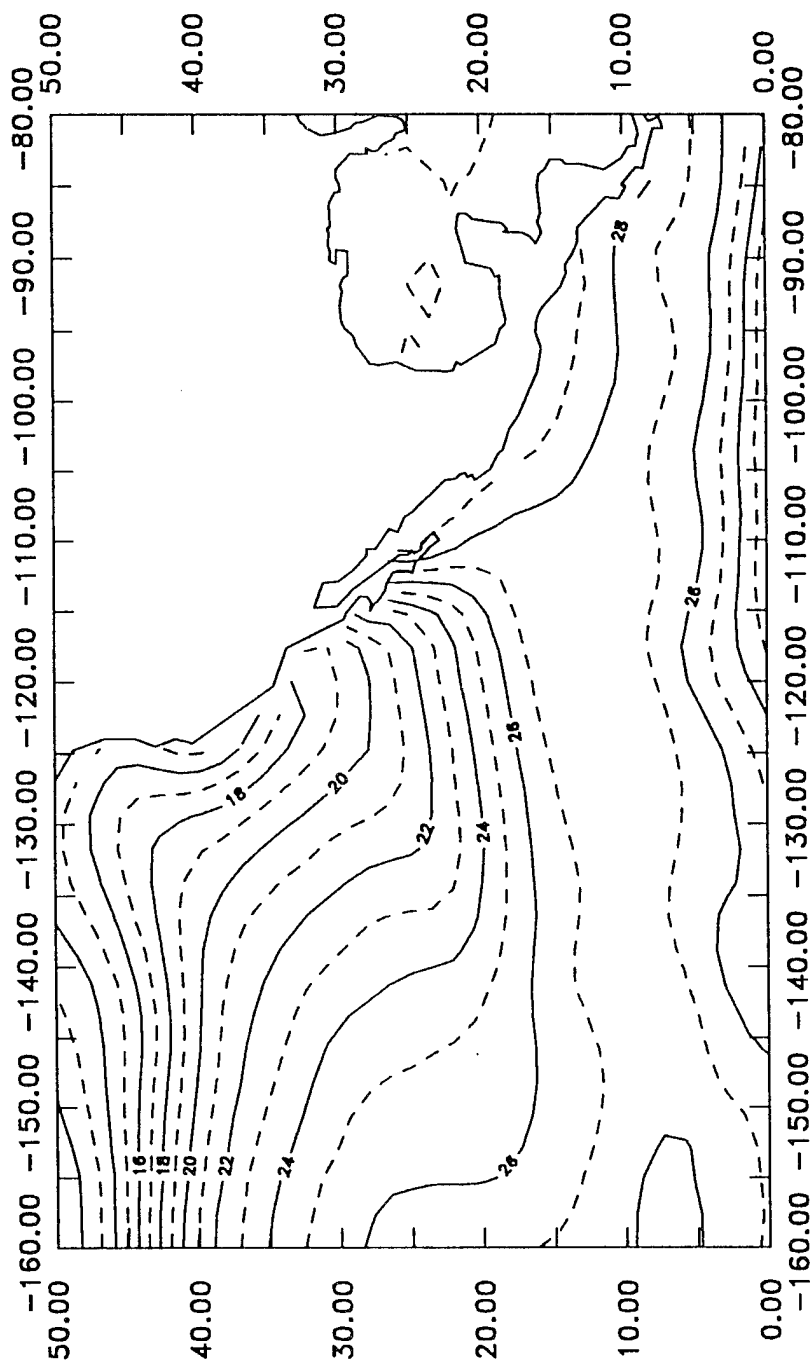


FIG. 30. Climatological sea surface temperatures for the month of September.

OCTOBER CLIMATOLOGICAL SST

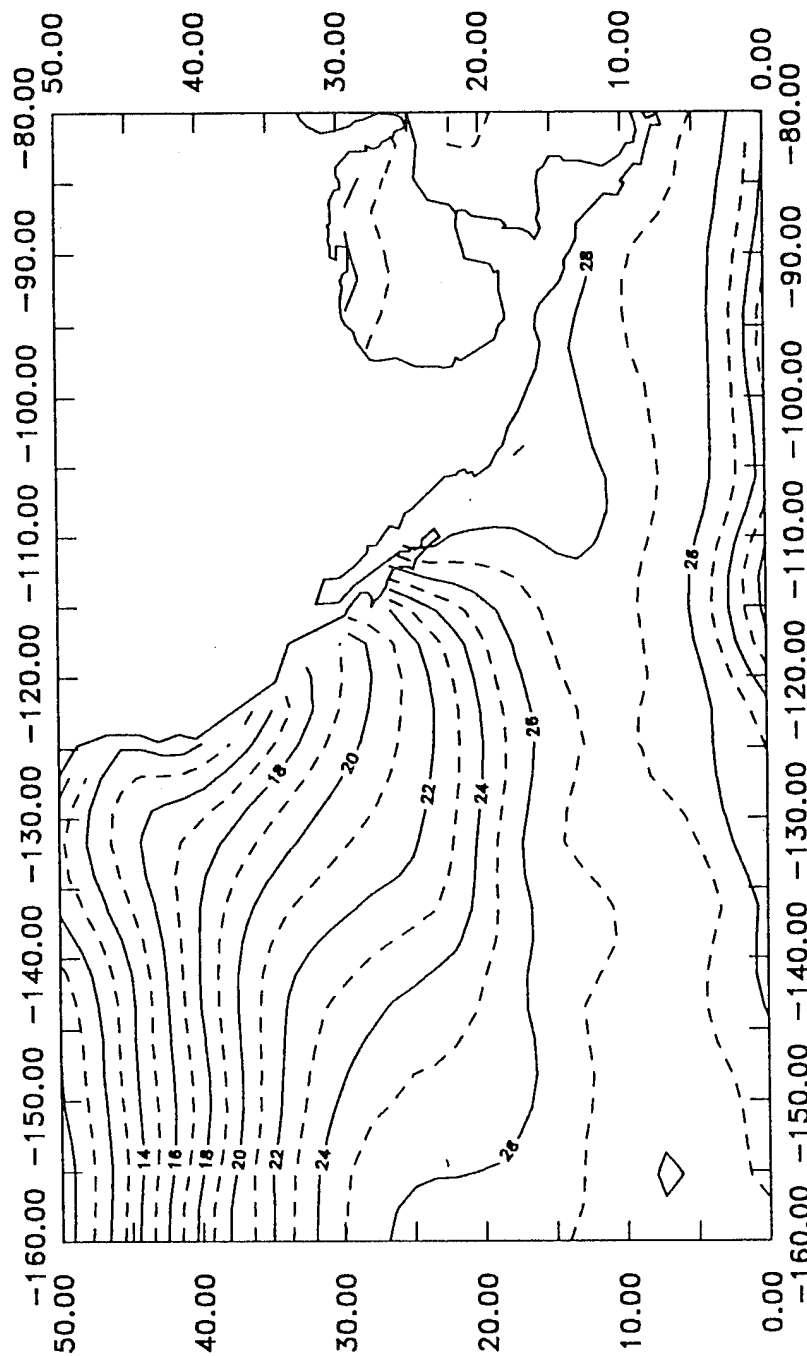


FIG. 31. Climatological sea surface temperatures for the month of October.

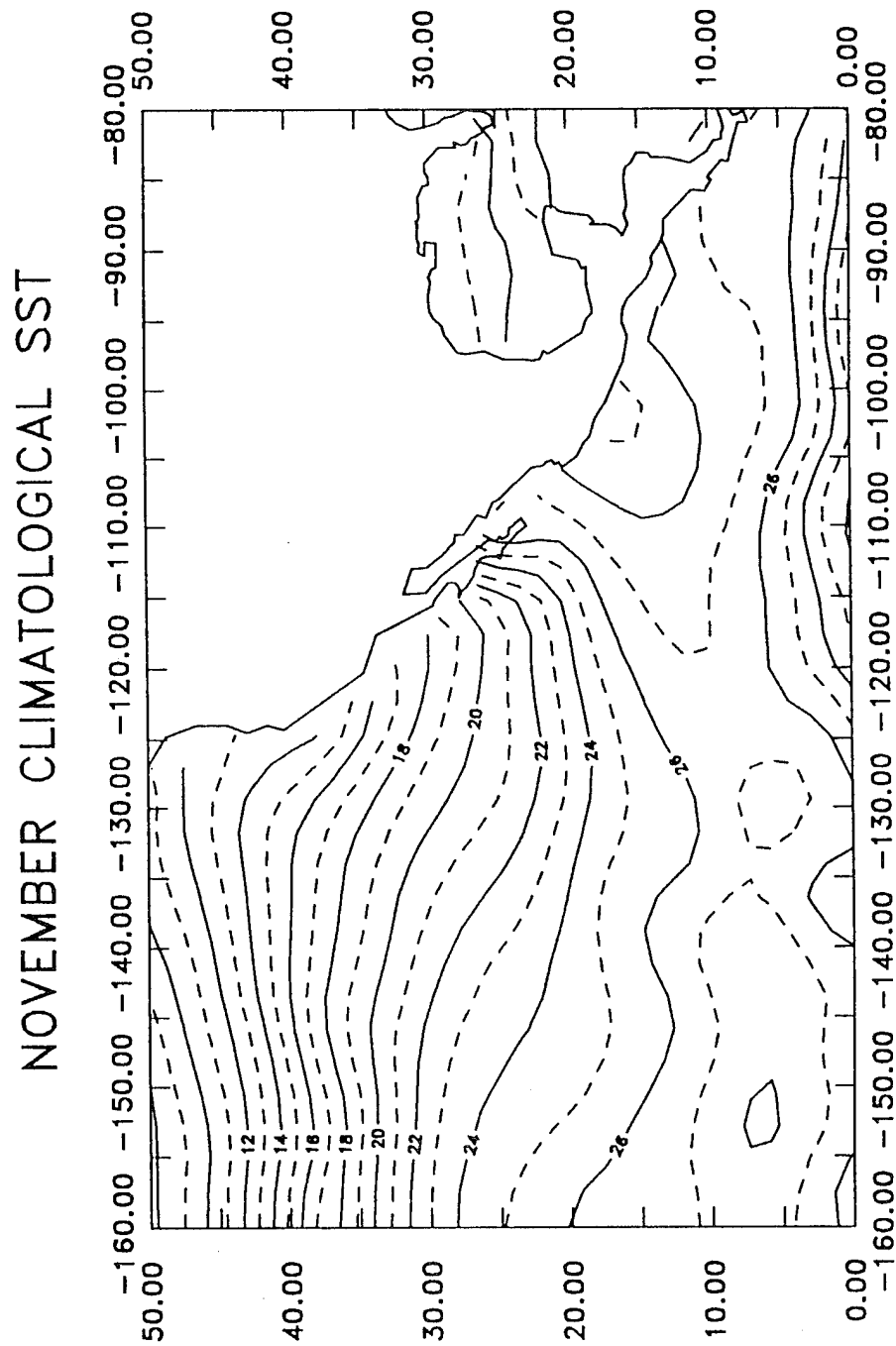


FIG. 32. Climatological sea surface temperatures for the month of November.

DECEMBER CLIMATOLOGICAL SST

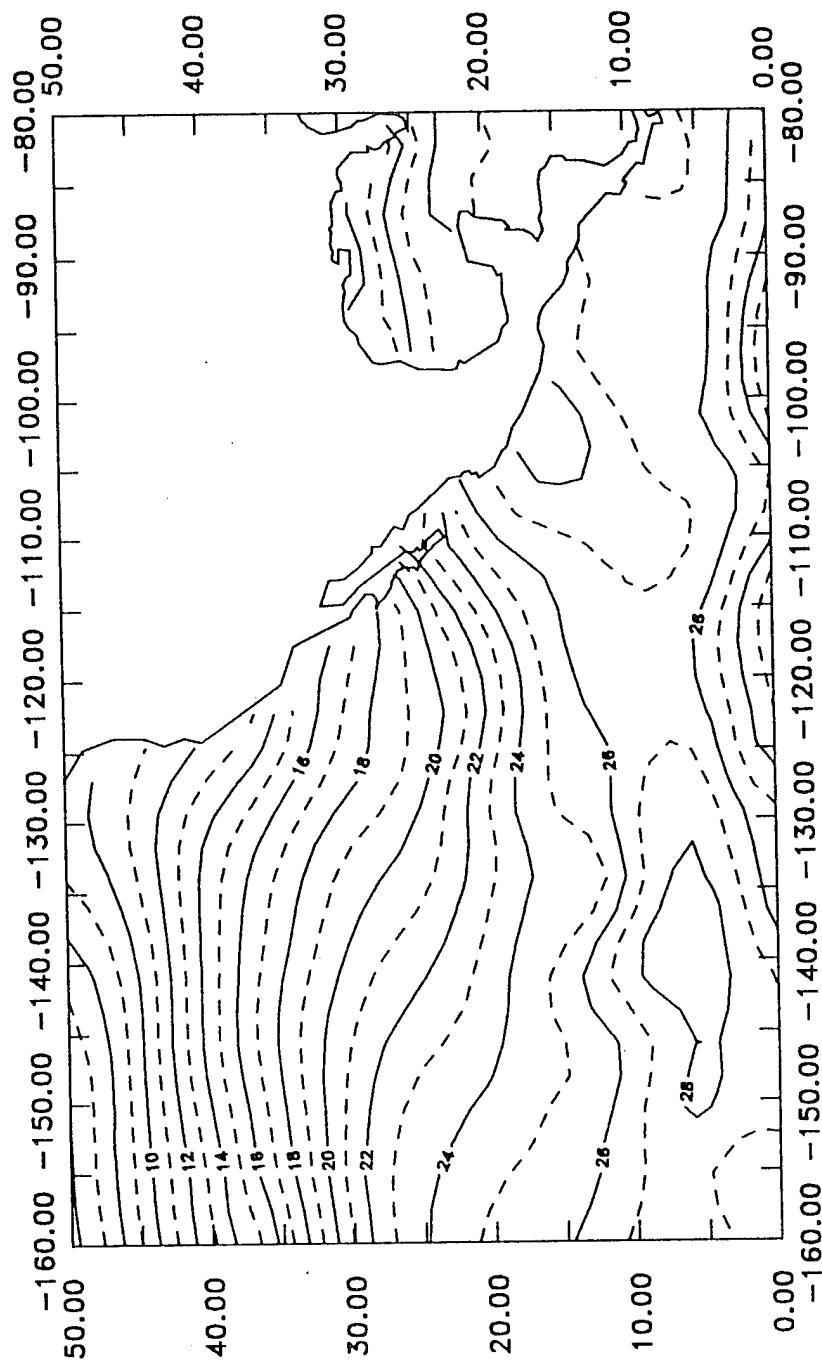


FIG. 33. Climatological sea surface temperatures for the month of December.

APPENDIX B

**TABLES OF SST GROUP PROPERTIES
STRATIFIED BY LATITUDE AND LONGITUDE**

TABLE 11. SST Group Properties for Eastern North Pacific tropical cyclones at positions $\geq 18^\circ\text{N}$.

SST Midpoint ($^\circ\text{C}$)	Number of Observations	Avg SST ($^\circ\text{C}$)	Avg Intensity (m/s)	Max Intensity (m/s)
19	52	18.8	10.8	20.1
20	58	20.0	11.7	26.1
21	141	21.0	14.6	36.2
22	282	22.0	14.5	39.1
23	465	23.0	16.6	43.5
24	632	23.9	19.4	51.5
25	620	24.9	23.2	58.7
26	461	25.9	25.3	59.5
27	388	26.9	25.9	56.8
28	394	28.0	25.8	59.0
29	182	28.9	23.8	55.5

TABLE 12. SST Group Properties for Eastern North Pacific tropical cyclones at positions south of 18°N .

SST Midpoint ($^\circ\text{C}$)	Number of Observations	Avg SST ($^\circ\text{C}$)	Avg Intensity (m/s)	Max Intensity (m/s)
19	0	0.0	0.0	0.0
20	0	0.0	0.0	0.0
21	0	0.0	0.0	0.0
22	0	0.0	0.0	0.0
23	7	23.2	10.9	17.7
24	68	24.1	17.8	50.8
25	303	25.1	22.8	56.3
26	795	26.0	24.2	61.1
27	1654	27.0	23.2	65.5
28	2904	27.9	20.2	66.5
29	1656	28.8	18.8	60.7

TABLE 13. SST Group Properties for Eastern North Pacific tropical cyclones at postions $\geq 110^{\circ}\text{W}$.

SST Midpoint ($^{\circ}\text{C}$)	Number of Observations	Avg SST ($^{\circ}\text{C}$)	Avg Intensity (m/s)	Max Intensity (m/s)
19	52	18.8	10.8	20.1
20	58	20.0	11.7	26.1
21	141	21.0	14.6	36.2
22	282	22.0	14.5	39.1
23	472	23.0	16.5	43.5
24	700	24.0	19.2	51.5
25	922	25.0	23.1	58.7
26	1243	26.0	24.6	61.1
27	1898	27.0	24.2	65.5
28	1504	27.7	22.4	66.5
29	6	28.8	23.8	32.7

TABLE 14. SST Group Properties for Eastern North Pacific tropical cyclones at postions east of 110°W .

SST Midpoint ($^{\circ}\text{C}$)	Number of Observations	Avg SST ($^{\circ}\text{C}$)	Avg Intensity (m/s)	Max Intensity (m/s)
19	0	0.0	0.0	0.0
20	0	0.0	0.0	0.0
21	0	0.0	0.0	0.0
22	0	0.0	0.0	0.0
23	0	0.0	0.0	0.0
24	0	0.0	0.0	0.0
25	1	25.4	11.9	11.9
26	13	26.0	21.7	42.7
27	149	27.1	17.4	55.6
28	1794	28.1	19.6	64.1
29	1832	28.8	19.3	60.7

LIST OF REFERENCES

- Ahrens, D. C., 1991: *Meteorology Today*. West Publishing Company, St. Paul, MN., 576 pp.
- Allard, R. A., 1984: A climatology of the characteristics of tropical cyclones in the Northeast Pacific during the period 1966-1980. Master of Science Thesis, Texas Tech. University, 106 pp.
- Bender, M. A., 1993: Numerical simulations of tropical cyclone-ocean interaction with a high-resolution coupled model. *J. Geo. Res.*, **98**, 23245-23262.
- DeMaria, M., and J. Kaplan, 1994a: Sea surface temperature and the maximum intensity of Atlantic tropical cyclones. *J. Climate*, **7**, 1325-1334.
- , and —, 1994b: A statistical hurricane intensity prediction scheme (SHIPS) for the Atlantic basin. *Wea. Forecasting*, **9**, 209-220.
- , J. J. Baik and J. Kaplan, 1993: Upper-level eddy angular momentum fluxes and tropical cyclone intensity change. *J. Atmos. Sci.*, **50**, 1133-1147.
- Dvorak, V. F., 1984: Tropical cyclone intensity analysis using satellite dat. NOAA Tech. Rep. NESDIS-11, 47 pp.
- Elsberry, R. L., E. L. Weniger and D. H. Meanor, 1988: A statistical tropical cyclone intensity forecast technique incorporating environmental wind and vertical wind shear information. *Mon. Wea. Rev.*, **116**, 2142-2154.
- Elsberry, R. L., W. M. Frank, G. J. Holland, J. D. Jarrell and R. L. Southern, 1987: *A Global View of Tropical Cyclones*. U. S. Office of Naval Research, Marine Meteorology Program. 185 pp.
- Emanuel, K. A., 1986: An air-sea interaction theory for tropical cyclones. Part I: Steady-state maintenance. *J. Atmos. Sci.*, **43**, 585-604.

- , 1988: The maximum intensity of hurricanes. *J. Atmos. Sci.*, **45**, 1143-1155.
- Evans, J. L., 1993: Sensitivity of tropical cyclone intensity to sea surface temperature. *J. Climate.*, **6**, 1133-1141.
- Fedorov, K. N., A. A. Varfolomeev, A. I. Ginzburg, A. G. Zatsepin, A. Yu. Krasnopevtsev, A. G. Ostrovsky and V. E. Skylarov, 1979: Thermal reaction of the ocean on the passage of the hurricane Ella. *Okeanologiya*, **19**, 992-1001.
- Fett, R. W., 1966: Upper-level structure of the formative tropical cyclone. *Mon. Wea. Rev.*, **94**, 9-18.
- Fisher, E. L., 1958: Hurricanes and the sea-surface temperature field. *J. Meteor.*, **15**, 328-333.
- Fritz, S., L. F. Hubert, and A. Timchalk, 1966: Some inferences from satellite pictures of tropical disturbances. *Mon. Wea. Rev.*, **94**, 231-236.
- Gray, W. M., 1968: Global view of the origin of tropical disturbances and storms. *Mon. Wea. Rev.*, **96**, 55-73.
- , 1984: Atlantic seasonal hurricane frequency. Part I: El Niño and 30 mb quasi-biennial oscillation influences. *Mon. Wea. Rev.*, **112**, 1649-1668.
- , C. W. Landsea, P. W. Mielke, and K. J. Berry, 1993: Predicting Atlantic basin seasonal tropical cyclone activity by 1 August. *Wea. Forecasting*, **8**, 73-86.
- , C. W. Landsea, P. W. Mielke, and K. J. Berry, 1994: Predicting Atlantic basin seasonal tropical cyclone activity by 1 June. *Wea. Forecasting*, **9**, 103-115.
- Halpert, M. S., and C. F. Ropelewski, 1989: Atlas of tropical sea surface temperature and surface winds. NOAA Atlas No. 8, U.S. Dept. of Commerce, Washington D. C., 13 pp.
- Haurwitz, B., 1935: The height of tropical cyclones and the eye of the storm. *Mon. Wea. Rev.*, **63**, 45-49.
- Hastenrath, S., 1985: *Climate and Circulation of the Tropics*. D. Reidel Publishing Company., 455 pp.
- Holliday, C. R., and A. H. Thompson, 1979: Climatological characteristics of rapidly intensifying typhoons. *Mon. Wea. Rev.*, **107**, 1022-1034.

- James, M. L., G. M. Smith and J. C. Wolford, 1985: *Applied Numerical Methods For Digital Computation*. Harper and Row, New York.
- Jordan, C. L., 1964: On the influence of tropical cyclones on the sea surface temperature. *Proc. Symp. Tropical Meteorology*, Wellington, New Zealand Meteor. Serv., 614-622.
- Knaff, J. A., 1993: Evidence of a stratospheric QBO modulation of tropical convection. Atmospheric Sciences Paper No. 520, Colorado State University, Ft. Collins, CO, 91 pp.
- Leipper, D. F., 1967: Observed ocean conditions and hurricane Hilda, 1964. *J. Atmos. Sci.*, **24**, 182-196.
- Levitus, S., 1982: *Climatological Atlas of the World Ocean*. NOAA Prof. Paper 13, 173 pp. [Available from the U.S. Government Printing Office, Washington, DC 20402.]
- Malkus, J. S., and H. Riehl, 1960: On the dynamics and energy transformations in steady-state hurricanes. *Tellus*, **12**, 1-20.
- Merrill, R. T., 1988: Environmental influences on hurricane intensification. *J. Atmos. Sci.*, **45**, 1678-1687.
- , 1987: An experiment in statistical prediction of tropical cyclone intensity change. NOAA Tech. Memo. NWS NHC-34, 34 pp.
- Miller, B. I., 1958: On the maximum intensity of hurricanes. *J. Meteor.*, **15**, 184-195.
- Molinari, J., and D. Vollaro, 1989: External influences on hurricane intensity. Part I: Outflow layer eddy angular momentum fluxes. *J. Atmos. Sci.*, **46**, 1093-1105.
- Newell, E. N., J. W. Kidson and D. G. Vincent, 1972: *The General Circulation of the Tropical Atmosphere*, Vol 1. The MIT Press, 258 pp.
- Ooyama, K., 1969: Numerical simulation of the life cycle of tropical cyclones. *J. Atmos. Sci.*, **26**, 3-40.
- Palmén, E., 1948: On the formation and structure of tropical hurricanes. *Geophysica*, **3**, 26-38.
- , and C. W. Newton, 1969: *Atmospheric Circulation Systems: Their Structure and Physical Interpretation*. Academic Press, New York and London, 603 pp.

- Perlroth, I., 1962: Relationship of central pressure of hurricane Esther (1961) and the sea surface temperature field. *Tellus*, **14**, 403-408.
- Philander, S. G., 1990: *El Niño, La Niña, and the Southern Oscillation*. Academic Press, San Diego, California, 293 pp.
- Price, J. F., 1981: Upper ocean response to a hurricane. *J. Phys. Oceanogr.*, **11**, 153-175.
- Pudov, V. D., A. A. Varfolomeev and K. N. Fedorov, 1979: Vertical structure of the wake of a typhoon in the upper ocean. *Okeanologiya*, **21**, 142-146.
- Ramage, C. S., and A. M. Hori, 1981: Meteorological aspects of El Niño. *Mon. Wea. Rev.*, **109**, 1827-1835.
- Rasmusson, E. M., and T. H. Carpenter, 1982: Variations in tropical sea surface temperature and surface wind fields associated with the southern oscillation/El Niño. *Mon. Wea. Rev.*, **110**, 354-384.
- Riehl, H., 1954: *Tropical Meteorology*. McGraw-Hill, 392 pp.
- Reid, G. C., and K. S. Gage, 1981: On the annual variation in height of the tropical tropopause. *J. Atmos. Sci.*, **38**, 1928-1938.
- Sadler, J. C., 1975: The upper tropospheric circulation over the global tropics. Dept. of Meteorology, Atlas UHMET 75-05, University of Hawaii, Honolulu, Hawaii.
- Schade, L. R., 1993: On the effect of ocean feedback on hurricane intensity. Preprints, *20th Conf. on Hurricanes and Tropical Meteorology*, Miami, FL, Amer. Meteor. Soc., 571-573.
- Shapiro, L. J., 1989: The relationship of the quasi-biennial oscillation to Atlantic tropical storm activity. *Mon. Wea. Rev.*, **117**, 1545-1552.
- Shay, L. K., P. G. Black, A. J. Mariano, J. D. Hawkins, and R. L. Elsberry, 1992: Upper ocean response to Hurricane Gilbert. *J. Geophys. Res.*, **97**, 20227-20248.
- Willoughby, H. E., J. A. Clos and M. G. Shoreibah, 1982: Concentric eyewalls, secondary wind maxima, and the evolution of the hurricane vortex. *J. Atmos. Sci.*, **39**, 395-411.
- Wright, R., 1969: Temperature structure across the Kuroshio before and after Typhoon Shirley. *Tellus*, **21**, 409-413.
- Zehnder, J. A., 1993: The influence of large-scale topography on barotropic vortex motion. *J. Atmos. Sci.*, **50**, 2519-2532.